JOURNAL OF GEOPHYSICAL RESEARCH, VOL. 91, NO. D9, PAGES 9807–9826, AUGUST 20, 1986

Chemistry of OH in Remote Clouds and Its Role in the Production of Formic Acid and Peroxymonosulfate

DANIEL J. JACOB

Center for Earth and Planetary Physics, Harvard Univerity, Cambridge, Massachusetts

The chemistry of OH in a remote nonprecipitating tropical cloud is studied with a coupled gas-phase and aqueous-phase chemical model. The model takes into account the radial dependence of the concentrations of short-lived aqueous-phase species, in particular, O_3(aq) and OH(aq). The radical OH(aq) is produced rapidly by the aqueous-phase reactions $O_2^- + O_3$ and $H_2O_2 + h\nu$ and is removed primarily by oxidation of $H_2C(OH)_2$, H_2O_2, and $HCOO^-$. Gas-droplet transfer of OH must be modeled as a reversible process, that is, the droplets cannot be assumed to be diffusion-limited OH(g) sinks. A strong OH(aq) concentration gradient exists between the surface and the interior of the droplets. The concentration of OH(aq) is strongly dependent on *p*H but is only weakly dependent on the sticking coefficient, the droplet radius, or the liquid water content of the cloud. Formic acid is rapidly produced by the aqueous-phase reaction $H_2C(OH)_2$ + OH, but $HCOO^-$ is in turn rapidly oxidized by OH(aq). The HCOOH concentration in cloud is shown to be strongly dependent on cloud water *p*H; clouds with *p*H greater than 5 are not efficient HCOOH sources. A novel mechanism is proposed for the oxidation of S(IV) by OH(aq). The main product is predicted to be HSO_5^- (peroxymonosulfate). Peroxymonosulfate appears to be stable in remote clouds and could contribute a large fraction of total cloud water sulfur.

INTRODUCTION

The hydroxyl radical OH plays a central role in tropospheric chemistry. Reaction with OH in the gas phase constitutes the primary sink for a number of atmospheric species, such as CH_4 and CO. Oxidation of SO_2 and NO_2 by OH(g) plays an important role in producing H_2SO_4 and HNO_3, the main components of acidic precipitation [*Calvert and Stockwell*, 1984]. The chemistry of OH(g) in the remote troposphere under cloud-free conditions has been studied in detail [*Chameides and Tan*, 1981; *Logan et al.*, 1981; *National Research Council*, 1984], but much less attention has been paid to the chemistry of OH in clouds. Complications to the chemistry arise in a cloud because of gas-droplet transfer and aqueous-phase reactions. The aqueous-phase radical OH(aq) is a very strong oxidant; reactions of OH(aq) in cloud droplets may have important implications for the composition of cloud water and, more generally, for the chemical transformations of atmospheric species. The object of this paper is to provide a model description of the chemistry of OH(g) and OH(aq) in clouds and to discuss two globally important aqueous-phase processes involving OH(aq): the production of HCOOH and the oxidation of S(IV).

The chemistry of OH is tied to that of HO_2 and H_2O_2, and it is convenient to group these three species into a chemical family: odd hydrogen (odd H). The odd H species are interconverted in the gas phase by a number of fast reactions, which constitute the odd H cycle [cf. *Logan et al.*, 1981]. Cloud formation perturbs the gas-phase odd H cycle as a result of the scavenging of water-soluble species by the droplets. The odd H species are all soluble in water and cycle rapidly in the aqueous phase by reactions analogous to the reactions in the gas phase [*Chameides and Davis*, 1982; *Chameides*, 1984; *Schwartz*, 1984]. The radical OH(aq) produced in this aqueous-phase odd H cycle interacts with OH(g) by gas-droplet transfer and oxidizes reduced species in the aqueous phase at rates often approaching the diffusion limit [*Anbar and Neta*, 1967].

The reaction of OH(aq) with hydrated formaldehyde, $H_2C(OH)_2$, produces HCOOH [*Chameides*, 1984]. Formic acid has been identified as an important contributor to the acidity of precipitation at remote sites [*Keene et al.*, 1983]. Aqueous-phase production of HCOOH by the above reaction is considerably more rapid than gas-phase production by breakup of double-bonded hydrocarbons [*Stockwell and Calvert*, 1983] or by oxidation of CH_2O(g) by HO_2(g) [*Su et al.*, 1979]. Because of this aqueous-phase source, clouds have been proposed as a major global source of HCOOH in the troposphere [*Chameides*, 1984; *Adewuyi et al.*, 1984]. However, cloud droplets are also efficient sinks for HCOOH because of the very rapid oxidation of $HCOO^-$ by OH(aq). A major point of this paper will be to show that the concentration of HCOOH in cloud is strongly dependent on the cloud water *p*H.

Another important process involving OH(aq) is the oxidation of SO_2. Scavenging of SO_2 by cloud droplets, followed by aqueous-phase oxidation of S(IV), has been suggested to be the dominant mechanism for global production of H_2SO_4 in the troposphere [*Hegg*, 1985]. The most important aqueous-phase S(IV) oxidants in remote clouds are thought to be H_2O_2(aq), O_3(aq), and OH(aq) [*Chameides*, 1984]. The oxidation reactions with H_2O_2(aq) and O_3(aq) are well understood [*McArdle and Hoffmann*, 1983; *Hoigne et al.*, 1985; *Hoffmann*, 1986], but the mechanism of the chain reaction initiated by OH(aq) attack on S(IV) is more uncertain. *McElroy* [1986] has recently pointed out major faults in the mechanisms assumed by previous cloud chemistry models. I will develop here a novel mechanism for the oxidation of S(IV) by OH(aq) which is consistent with currently available kinetic data. A major feature of this mechanism is that the chain carrier intermediate SO_5^- may oxidize other species besides S(IV), thereby terminating the oxidation chain. The main product is predicted to be HSO_5^- (peroxymonosulfate). I will argue that HSO_5^- may be a stable sulfur species in remote clouds and may constitute an important fraction of total cloud water sulfur.

Paper number 6D0268.
0148-0227/86/006D-0268$05.00

The discussion will be based on a detailed gas-phase/aqueous-phase chemical model simulating the chemistry of a nonprecipitating cloud in the remote troposphere. An innovative feature of the model is its treatment of the radial dependence of the concentrations of short-lived aqueous-phase species, in particular, OH(aq). The concentration of OH(aq) at the droplet surface may differ considerably from that in the droplet interior, and this has important implications in determining the OH(aq) volatilization flux. Previous models of cloud water chemistry have assumed that the droplets constitute diffusion-limited sinks for OH(g) [*Chameides and Davis*, 1982; *Chameides*, 1984; *Seigneur et al.*, 1985]; however, OH(g) is only moderately soluble in water, with a Henry's law constant of about 20 M atm^{-1}. Therefore gas-droplet transfer of OH must be modeled as a reversible process in which both the absorption flux and the volatilization flux are considered. An analytical solution for the OH(aq) radial concentration profile will be presented, which can easily be incorporated into complex cloud chemistry models.

CLOUD CHEMISTRY MODEL

Cloud Formation

Cloud formation is simulated by isobaric cooling of a boundary layer air parcel in a tropical spring atmosphere. The standard model conditions are listed in Tables 1*a* and 1*b*. The temperature of the air parcel is assumed to drop instantaneously from its initial value (297 K) down to a value at which a specified liquid water content (5×10^{-7} vol/vol in the standard simulation) is produced by condensation on preexisting nuclei. The cloud droplets are assumed to be monodisperse and to reach instantaneously a droplet radius fixed by input to the model (10 μm in the standard simulation). The droplets do not precipitate and follow the air parcel with negligible inertia.

The radiation field is initially calculated for clear noontime conditions, with the parameters of Table 1*a*. Cloud formation enhances radiation in the upper region of the cloud (because of scattering from below) and weakens radiation in the lower region of the cloud (because of increased optical depth). An intermediate level is considered where cloud formation causes no net change in the radiation field; sensitivity analyses are conducted to examine the effect of insolation changes.

TABLE 1*a*. Standard Model Conditions: Model Parameters

Parameter	Value
Latitude	15°
Solar declination	0°
Suface albedo	0.07
Temperature	
Before cloud formation	297 K
In cloud	293 K
Relative humidity	
Before cloud formation	80%
In cloud	100%
Liquid water content	0.5 g m^{-3} (5×10^{-7} vol/vol)
Droplet radius	10μm
Sticking coefficient	0.1
Condensation nuclei	7×10^{-9} moles m^{-3} NaCl,[a] [from *Gillette and Blifford*, 1971]

Radiation field is calculated for clear-sky conditions. Values for vertical columns of ozone, water vapor, and aerosol are from *Logan et al.* [1981].

[a]H^+ or OH^- are added in pH sensitivity calculations.

TABLE 1*b*. Standard Model Conditions: Initial Concentrations of Gas-Phase Species Before Cloud Formation

Long-Lived Species[a]	Concentration, ppb	Reference
CH_4	1700	*Logan et al.* [1981]
CO	140	*Logan et al.* [1981]
Odd nitrogen	0.2	*Logan et al.* [1981]
O_3	25	*Logan et al.* [1981]
C_2H_4	0.2	*Rudolph and Ehhalt* [1981]
HCl	0.5	*Vierkorn-Rudolph et al.* [1984]
CH_3OH[b]	0.8	*Cavanagh et al.* [1969]
SO_2[b]	0.1	*Maroulis et al.* [1980]
NH_3[b]	0.05	*Ayers and Gras* [1983]

Other species[c]	Concentration, molecules cm^{-3}
CH_2O	1.3(10)
CH_3O_2	3.9(8)
CH_3OOH	1.9(10)
NO	2.6(8)
NO_2	6.4(8)
NO_3	5.4(4)
N_2O_5	7.3(2)
HNO_3	4.0(9)
HNO_2	6.1(6)
HNO_4	6.6(6)
OH	5.2(6)
HO_2	5.8(8)
H_2O_2	8.3(10)
HCOOH	1.1(8)

Read 1.3(10) as 1.3×10^{10}.

[a]Concentrations of these species are held at a fixed value throughout the simulation.

[b]Concentrations of these species are held at a fixed value only in the absence of cloud (see text).

[c]Initial concentrations of these species are calculated from the concentrations of long-lived species by iteration of the gas-phase mechanism over successive diurnal cycles (see text).

Gas-Phase Chemical Mechanism

A standard gas-phase mechanism for the H_xO_y-N_xO_y-CH_4-CO system is used, which includes over 100 reactions. The reader is referred to *Logan et al.* [1981] for a detailed discussion of this mechanism. Rate constants have been updated following the recommendations of the *Jet Propulsion Laboratory* [1983]. The radical OH(g) is produced by

(RG1) $$O_3 + h\nu \rightarrow O_2 + O(^1D)$$

followed by

(RG2) $$O(^1D) + H_2O \rightarrow 2OH$$

and by

(RG3) $$H_2O_2 + h\nu \rightarrow 2OH$$

Reactions of HO_2(g) with O_3 and NO may also be important:

(RG4) $$HO_2 + O_3 \rightarrow OH + 2O_2$$

RG5) $$HO_2 + NO \rightarrow OH + NO_2$$

Removal of OH(g) is mostly by reactions with CH_4 and CO:

(RG6) $$CH_4 + OH \xrightarrow{O_2} CH_3O_2 + H_2O$$

(RG7) $$CO + OH \xrightarrow{O_2} CO_2 + HO_2$$

where it is assumed that CH_3(g) and H(g) radicals react instantaneously with O_2 to give the indicated products.

TABLE 2a. Aqueous-Phase Chemistry: Henry's Law Constants

Reaction No.	Species	$K_{H,298}$, M atm^{-1}	ΔH_{298}°, kcal mol^{-1}	Reference
(H1)	O_3	1.10(−2)	−4.8	*Hoffmann and Calvert* [1985]
(H2)	OH	2.5(1)	−10.5[a,b]	*National Bureau of Standards* [1971]; *Klaning et al.* [1985]
(H3)	HO_2	2.(3)	−13.2[a]	*Schwartz* [1984]
(H4)	H_2O_2	7.4(4)	−13.2	*Lind and Kok* [1986]
(H5)	CH_3O_2	6.(0)[a]	−11.2[a]	see footnote[c]
(H6)	CH_3OOH	2.2(2)	−11.2	*Lind and Kok* [1986]
(H7)	CH_3OH	2.2(2)	−9.8	*Snider and Dawson* [1985]
(H8)	CH_2O	6.3(3)[d]	−12.9	*Ledbury and Blair* [1925]
(H9)	HCOOH	3.7(3)[e]	−11.4	*Latimer* [1952]
(H10)	CO_2	3.4(−2)	−4.85	*Hoffman and Calvert* [1985]
(H11)	NO	1.9(−3)	−2.94	*Schwartz and White* [1981]
(H12)	HNO_2	4.9(1)	−9.5	*Schwartz and White* [1981]
(H13)	NO_2	1.2(−2)	−5.0	*Schwartz and White* [1981]
(H14)	N_2O_5	∞[a]		
(H15)	NO_3	2.1(5)[a]	−17.3[a]	K_{H19}
(H16)	SO_2	1.2(0)	−6.27	*Hoffman and Calvert* [1985]
(H17)	NH_3	7.4(1)	−6.80	*Hales and Drewes* [1979]

Reaction No.	Reaction	$K_{H,298}$, M^2 atm^{-1}	ΔH_{298}°, kcal mol^{-1}	Reference
(H18)	$HCl(g) = H^+ + Cl^-$	2.05(6)	−18.	*Hoffman and Calvert* [1985]
(H19)	$HNO_3(g) = H^+ + NO_3^-$	3.3(6)	−17.3	*Schwartz and White* [1981]

Read 1.10(−2) as 1.10×10^{-2}.
[a]Estimated value.
[b]Assumed to be the same as for H_2O [*Latimer*, 1952].
[c]The relation $K_{H5} = K_{H6}(K_{H3}/K_{H4})$ is assumed.
[d]Equilibrium $CH_2O(g) \rightleftharpoons H_2C(OH)_2$.
[e]$K_{H9} = 5.6 \times 10^3$ M atm^{-1} [*Chao and Zwolinski*, 1978; *Wagman et al.*, 1982] is considered in a sensitivity calculation (see text).

The species HCOOH(g) has been added to the gas-phase chemical mechanism of *Logan et al.* [1981] because of its importance in cloud. It is produced in the gas phase by addition of HO_2(g) to CH_2O(g) [*Su et al.*, 1979; *Atkinson and Lloyd*, 1984]:

$$\text{(RG8)} \quad CH_2O + HO_2 \leftrightarrows O_2CH_2OH$$
$$K = 6.7 \times 10^{-15} \text{ cm}^3$$

$$\text{(RG9)} \quad O_2CH_2OH + HO_2 \rightarrow HCOOH + H_2O + O_2$$
$$k = 2 \times 10^{-12} \text{ cm}^3 \text{ s}^{-1}$$

$$\text{(RG10)} \quad O_2CH_2OH + NO \xrightarrow{O_2} HCOOH + NO_2 + HO_2$$
$$k = 7 \times 10^{-12} \text{ cm}^3 \text{ s}^{-1}$$

$$\text{(RG11)} \quad O_2CH_2OH + O_2CH_2OH \xrightarrow{O_2} 2HCOOH + 2HO_2$$
$$k = 1.2 \times 10^{-13} \text{ cm}^3 \text{ s}^{-1}$$

and is also a low-yield product of the gas-phase reaction of C_2H_4 with O_3. The stoichiometry proposed by *Chameides* [1984] was adopted here:

$$\text{(RG12)} \quad C_2H_4 + O_3 \rightarrow \text{multiple steps} \rightarrow CH_2O + 0.3(H_2O + CO) + 0.04HCOOH + 0.2(CO_2 + H_2) + 0.1(CO_2 + 2H)$$
$$k = 2.6 \times 10^{-14} \exp(-2828/T) \text{ cm}^3 \text{ s}^{-1}$$

The gas-phase sink for HCOOH(g) is reaction with OH(g) [*Zetzsch and Stuhl*, 1982]:

$$\text{(RG13)} \quad HCOOH + OH \xrightarrow{O_2} CO_2 + HO_2 + H_2O$$
$$k = 3.2 \times 10^{-13} \text{ cm}^3 \text{ s}^{-1}$$

The species CH_3OH(g), SO_2(g), and NH_3(g) have also been added to the gas-phase mechanism. These species have fairly long lifetimes (several days) against oxidation by OH(g), their main gas-phase chemical sink; in a cloud, however, they may be rapidly depleted by gas-droplet transfer. Their concentrations are held at a fixed value under cloud-free conditions, and this constraint is relaxed upon cloud formation to allow them to be scavenged by the cloud droplets.

Aqueous-Phase Chemical Mechanism

The aqueous-phase chemical mechanism is given in Table 2. The mechanism draws from the earlier work of *Graedel and Wechsler* [1981], *Chameides and Davis* [1982], *Jacob and Hoffmann* [1983], *Graedel and Goldberg* [1983], *Chameides* [1984], and *Hoffmann and Calvert* [1985]. A number of reactions have been added to the above mechanisms, and rate constants have been updated based on recent literature. Rates and equilibrium constants were estimated for reactions for which no data are available. Reactions that are too slow to affect the chemistry over the lifetime of a cloud were generally excluded from Table 2c, although a few of these reactions are listed to stress that the reaction in question is indeed slow. These slow reactions are indicated by footnote *d* (Table 2c.) The reactions of

TABLE 2b. Aqueous-Phase Chemistry: Aqueous-Phase Equilibrium Constants

Reaction No.	Reaction	K_{298} M^n	ΔH_{298}°, kcal mol^{-1}	Reference
(RA1)	$H_2O = H^+ + OH^-$	1.00(−14)	13.34	*Hoffmann and Calvert* [1985]
(RA2)	$HO_2 = H^+ + O_2^-$	2.05(−5)	0.[a]	*Bielski* [1978]
(RA3)	$H_2O_2 = H^+ + HO_2^-$	1.58(−12)	7.4	*Hoffmann and Calvert* [1985]
(RA4)	$HCOOH = H^+ + HCOO^-$	1.78(−4)	0.3	*Sillen and Martell* [1964]
(RA5)	$HNO_2 = H^+ + NO_2^-$	5.1(−4)	2.5	*Schwartz and White* [1981]
(RA6)	$H_2CO_3 = H^+ + HCO_3^-$	4.4(−7)	2.0	*Hoffmann and Calvert* [1985]
(RA7)	$SO_2 \cdot H_2O = H^+ + HSO_3^-$	1.3(−2)	−4.0	*Hoffmann and Calvert* [1985]
(RA8)	$HSO_3^- = H^+ + SO_3^{2-}$	6.31(−8)	−2.99	*Hoffmann and Calvert* [1985]
(RA9)	$NH_3 \cdot H_2O = NH_4^+ + OH^-$	1.7(−5)	0.9	*Hoffmann and Calvert* [1985]
(RA10)	$CH_2O \underset{H_2O}{\rightleftharpoons} H_2C(OH)_2$	1.8(3)	−8.04	*Bell* [1966]
(RA11)	$Cl^- + Cl = Cl_2^-$	1.9(5)	0.[b]	*Jayson et al.* [1973]
(RA12)	$HOCH_2SO_3^- = {}^-OCH_2SO_3^- + H^+$	2.0(−12)	0.[b]	*Sorensen and Andersen* [1970]

Read 1.00(−14) as 1.00×10^{-14}.
[a] *Baxendale et al.* [1971].
[b] Estimated value.

CO_3^-, Cl_2^-, and aqueous-phase odd N species were included in the calculations for consistency with previous models but were found to play a negligible role in the droplet chemistry of interest here. They will not be discussed further.

Very few data are available for the activation energies E_a of aqueous-phase radical reactions. When no data were available, E_a was estimated from the rate constant k at 298 K and a typical value $A = 1. \times 10^{10}$ M^{-1} s^{-1} for the preexponential factor in the Arrhenius epression. A lower limit to the apparent activation energy of an aqueous-phase bimolecular reaction is the temperature dependence of the diffusion-controlled reaction, which corresponds to $E_a \approx 3$ kcal mol^{-1} in an Arrhenius formulation [*Glasstone et al.*, 1941]. If $A = 1 \times 10^{10}$ M^{-1} s^{-1} were assumed for reactions with $k > 7 \times 10^7$ M^{-1} s^{-1}, activation energies below this lower limit would be predicted; instead, $E_a = 3$ kcal mol^{-1} was assumed for all reactions with $k > 7 \times 10^7$ M^{-1} s^{-1}. Estimates of E_a by the above method are consistent with experimental data for the two aqueous-phase radical reactions in Table 2c for which data are available: $E_a = 4.7$ kcal mol^{-1} and log $A = 9.8$ for $HO_2 + HO_2$ [*Thomas and Ingold*, 1968], and $E_a = 3.4$ kcal mol^{-1} and log $A = 9.9$ for $OH + H_2O_2$ [*Christensen et al.*, 1982].

The focus of discussion in this paper is the chemistry of a mature cloud, 1 hour after cloud formation. The assumption that the newly formed cloud droplets reach a stable 10-μm radius "instantaneously" must be discussed from this standpoint. The time required for activated nuclei to reach such a size under typical supersaturated conditions is of the order of a minute [*Pruppacher and Klett*, 1978]. Scavenging of soluble gases by the cloud droplets proceeds on a similar time scale [*Levine and Schwartz*, 1982; *Jacob*, 1985]. During the first few minutes of cloud formation, soluble gases are progressively depleted from the gas phase by the growing droplets; the rates of these transient processes cannot be simulated accurately by the model because no attempt is made to simulate droplet growth. However, the net result, that soluble gases are depleted during the first few minutes of cloud formation, is predicted properly. For the present purpose a precise determination of the actual rates at which transient chemical processes occur in the initially growing cloud is of no real importance. Past this initial period, changes in the chemical composition of the cloud proceed at a much slower pace.

Cloud water *p*H stabilizes within minutes following cloud formation and subsequently changes very little over the lifetime of the cloud. The main chemical processes controlling the *p*H are (1) the dissolution of condensation nuclei, (2) the scavenging of acidic and alkaline gases initially present in the air (HNO_3, SO_2, HCl, HCOOH, CO_2, NH_3), and (3) the oxidation of S(IV). All of these processes take place on a time scale of minutes [*Chameides*, 1984; *Jacob*, 1985]. Production of HCOOH in the aqueous phase proceeds over a longer time scale but is too small to have a significant effect on *p*H. When condensation takes place on neutral nuclei, as in the standard simulation, the cloud water *p*H is given to a good approximation by a balance of the major acidic (HNO_3, SO_2, HCl, HCOOH, CO_2) and alkaline (NH_3) species present in the atmosphere before cloud formation (Table 1b). If quantitative oxidation of SO_2 to H_2SO_4 is assumed [*Chameides*, 1984], the *p*H can be calculated readily. With the conditions of Table 1, one finds *p*H = 4.16.

This rather low *p*H value is due mostly to the scavenging of acidic gases, whose concentrations in the remote troposphere may vary considerably from the values given in Table 1b. The cloud water *p*H is also very sensitive to the acidity of the condensation nuclei. Therefore it is necessary to study the sensitivity of the calculations to the cloud water *p*H imposed by the initial conditions. A series of simulations were conducted where H^+ or OH^- were added to the neutral nuclei in various quantities to give cloud water *p*H values ranging from 3 to 7. This method for specifying the initial atmospheric acidity is somewhat artificial because it ignores the thermodynamic partitioning of the acidity between the gas phase and the aerosol phases [cf. *Jacob et al.*, 1986a, b]. However, modifying the acidity of the nuclei is for the present purpose equivalent to modifying the initial concentrations of acidic or alkaline gases, because these gases are rapidly scavenged upon cloud formation.

Gas-Droplet Transfer

Consider a gas-phase species i present in the cloud with concentration n_i (measured in molecules per cubic centimeter of air) and dissolving in the cloud droplets to give aqueous-phase species j with concentration C_j (M). Mass transport in clouds is controlled by molecular diffusion [*Schwartz*, 1986]. The absorption flux Φ_{in} (in molecules per cubic centimeter of air per second) of species i to the cloud droplets is given by

TABLE 2c. Aqueous-Phase Chemistry: Aqueous-Phase Reaction Rate Constants

Reaction No.	Reaction	k_{298}, M^n s^{-1}	E_a, kcal mol^{-1}	Reference
	Odd Hydrogen[a]			
(RA13)	$O_3 + h\nu \xrightarrow{H_2O} H_2O_2 + O_2$			*Graedel and Wechsler* [1981]
(RA14)	$H_2O_2 + h\nu \rightarrow 2OH$			*Graedel and Wechsler* [1981]
(RA15)	$OH + HO_2 \rightarrow H_2O + O_2$	7.(9)	3.[b]	*Sehested et al.* [1968]
(RA16)	$OH + O_2^- \rightarrow OH^- + O_2$	1.(10)	3.[b]	*Sehested et al.* [1968]
(RA17)	$OH + H_2O_2 \rightarrow H_2O + HO_2$	2.7(7)	3.4	*Christensen et al.* [1982]
(RA18)[d]	$OH + O_3 \rightarrow HO_2 + O_2$	2.(9)		*Staehelin et al.* [1984]
(RA19)	$OH + Cl^- + H^+ \rightarrow H_2O + Cl$	1.5(10)	3.[b]	*Jayson et al.* [1973]
(RA20)	$OH + HCO_3^- \rightarrow H_2O + CO_3^-$	1.5(7)	3.8[b]	*Weeks and Rabani* [1966]
(RA21)	$HO_2 + HO_2 \xrightarrow{H_2O} H_2O_2 + O_2$	8.6(5)	4.7[c]	*Bielski* [1978]
(RA22)	$HO_2 + O_2^- \rightarrow H_2O_2 + O_2 + OH^-$	1.(8)	3.[b]	*Bielski* [1978]
(RA23)[d]	$O_2^- + O_2^- \xrightarrow{2H_2O} H_2O_2 + O_2 + 2OH^-$	$<3(-1)$		*Bielski* [1978]
(RA24)[d]	$HO_2 + H_2O_2 \rightarrow OH + O_2 + H_2O$	$5.(-1)$		*Weinstein and Bielski* [1979]
(RA25)[d]	$O_2^- + H_2O_2 \rightarrow OH + O_2 + OH^-$	$1.3(-1)$		*Weinstein and Bielski* [1979]
(RA26)[d]	$HO_2 + O_3 \xrightarrow{H_2O} OH + 2O_2$	$<1.(4)$		*Sehested et al.* 1984]
(RA27)	$O_2^- + O_3 \rightarrow OH + 2O_2 + OH^-$	1.5(9)	3.[b]	*Sehested et al.* [1983]; *Buhler et al.* [1984]
(RA28)	$HO_2 + Cl_2^- \rightarrow O_2 + 2Cl^- + H^+$	4.5(9)	3.[b]	*Ross and Neta* [1979]
(RA29)	$O_2^- + Cl_2^- \xrightarrow{H_2O} O_2 + 2Cl^-$	1.(9)	3.[b]	*Ross and Neta* [1979]
(RA30)	$O_2^- + CO_3^- \rightarrow O_2 + HCO_3^- + OH^-$	4.(8)	3.[b]	*Behar et al.* [1970]
(RA31)	$O_3 + OH^- \xrightarrow{H_2O} H_2O_2 + O_2 + OH^-$	7.0(1)	11.[b]	*Staehelin and Hoigne* [1982]
(RA32)	$HO_2^- + O_3 \rightarrow OH + O_2^- + O_2$	2.8(6)	5.[b]	*Staehelin and Hoigne* [1982]
(RA33)	$H_2O_2 + CO_3^- \rightarrow HO_2 + HCO_3^-$	8.(5)	5.6[b]	*Behar et al.* [1970]
(RA34)	$H_2O_2 + Cl_2^- \rightarrow 2Cl^- + H^+ + HO_2$	1.4(5)	6.7[b]	*Hagesawa and Neta* [1978]
(RA35)	$OH^- + Cl_2^- \rightarrow 2Cl^- + OH$	7.3(6)	4.3[b]	*Hagesawa and Neta* [1978]
	CH_4 Oxidation Chain			
(RA36)	$CH_3O_2 + HO_2 \xrightarrow{H_2O} CH_3OOH + O_2$	4.3(5)[b]	6.[b]	$k_{A21}/2$
(RA37)	$CH_3O_2 + O_2^- \rightarrow CH_3OOH + O_2 + OH^-$	5.(7)[b]	3.2[b]	$k_{A22}/2$
(RA38)	$CH_3OOH + h\nu \xrightarrow{O_2} CH_2O + OH + HO_2$			*Graedel and Wechsler* [1981]
(RA39)	$CH_3OOH + OH \rightarrow CH_3O_2 + H_2O$	2.7(7)[b]	3.4[b]	k_{A17}
(RA40)	$CH_3OOH + OH \rightarrow CH_2O + OH + H_2O$	1.9(7)[b]	3.7[b]	see footnote[e]
(RA41)	$CH_3OH + OH \rightarrow CH_2O + HO_2 + H_2O$	4.5(8)	3.[b]	*Anbar and Neta* [1967]
(RA42)	$CH_3OH + CO_3^- \xrightarrow{O_2} CH_2O + HO_2 + HCO_3^-$	2.6(3)	9.[b]	*Chen et al.* [1973]
(RA43)	$CH_3OH + Cl_2^- \xrightarrow{O_2} CH_2O + HO_2 + H^+ + 2Cl^-$	3.5(3)	8.9[b]	*Hagesawa and Neta* [1978]
(RA44)	$H_2C(OH)_2 + OH \xrightarrow{O_2} HCOOH + HO_2 + H_2O$	2.(9)	3.[b]	*Anbar and Neta* [1967] *Bothe and Schulte-Frohlinde* [1980]
(RA45)[d]	$H_2C(OH)_2 + O_3 \xrightarrow{O_2}$ products	$1.(-1)$		*Hoigne and Bader* [1983*a*]
(RA46)	$HCOOH + OH \xrightarrow{O_2} CO_2 + HO_2 + H_2O$	2.(8)	3.[b]	*Anbar and Neta* [1967]
(RA47)	$HCOO^- + OH \xrightarrow{O_2} CO_2 + HO_2 + OH^-$	2.5(9)	3.[b]	*Anbar and Neta* [1967]
(RA48)[d]	$HCOOH + H_2O_2 \rightarrow HC(O)OOH + H_2O$	$4.6(-6)$	10.3	*Shapilov and Kostyukovskii* [1974]
(RA49)[d]	$HCOOH + O_3 \rightarrow CO_2 + OH + HO_2$	5.(0)		*Hoigne and Bader* [1983*b*]
(RA50)[d]	$HCOO^- + O_3 \rightarrow CO_2 + OH + O_2^-$	1.(2)		*Hoigne and Bader* [1983*b*]
(RA51)	$HCOO^- + CO_3^- \xrightarrow{H_2O, O_2} CO_2 + HCO_3^- + HO_2 + OH^-$	1.1(5)	6.8[b]	*Chen et al.* [1973]
(RA52)	$HCOOH + Cl_2^- \xrightarrow{O_2} CO_2 + HO_2 + 2Cl^- + H^+$	6.7(3)	8.5[b]	*Hagesawa and Neta* [1978]
(RA53)	$HCOO^- + Cl_2^- \xrightarrow{O_2} CO_2 + HO_2 + 2Cl^-$	1.9(6)	5.1[b]	*Hagesawa and Neta* [1978]
	Odd Nitrogen			
(RA54)	$HNO_2 + h\nu \xrightarrow{H_2O} NO + OH$			*Graedel and Wechsler* [1981]
(RA55)	$NO_2^- + h\nu \rightarrow NO + OH + OH^-$			*Graedel and Wechsler* [1981]
(RA56)	$HNO_2 + OH \rightarrow NO_2 + H_2O$	1.(9)	3.[b]	*Rettich* [1978]
(RA57)	$NO_2^- + OH \rightarrow NO_2 + OH^-$	1.(10)	3.[b]	*Treinin* [1970]
(RA58)	$HNO_2 + H_2O_2 + H^+ \rightarrow NO_3^- + 2H^+ + H_2O$	4.6(3)	13.8	*Damschen and Martin* [1983]
(RA59)	$NO_2^- + O_3 \rightarrow NO_3^- + O_2$	5.(5)	13.8	*Damschen and Martin* [1983]
(RA60)	$NO_2^- + NO_3 \rightarrow NO_2 + NO_3^-$	1.2(9)	3.[b]	*Daniels* [1968]

TABLE 2c. (continued)

Reaction No.	Reaction	k_{298}, M^n s^{-1}	E_a, kcal mol^{-1}	Reference
	Odd Nitrogen (continued)			
(RA61)	$NO_2^- + Cl_2^- \rightarrow NO_2 + 2Cl^-$	2.5(8)	3.[b]	*Hagesawa and Neta* [1978]
(RA62)	$NO_2 + OH \rightarrow NO_3^- + H^+$	1.3(9)	3.[b]	*Gratzel et al.* [1970]
(RA63)	$2NO_2 \xrightarrow{H_2O} HNO_2 + H^+ + NO_3^-$	1.(8)	3.[b]	*Lee and Schwartz* [1981]
(RA64)	$NO_2 + NO \xrightarrow{H_2O} 2H^+ + 2NO_2^-$	3.(8)	3.[b]	*Hoffmann and Calvert* [1985]
(RA65)	$NO_3^- + h\nu \xrightarrow{H_2O} NO_2 + OH + OH^-$			*Graedel and Wechsler* [1981]
(RA66)	$NO_3 + h\nu \rightarrow NO + O_2$			*Graedel and Wechsler* [1981]
(RA67)	$NO_3 + HO_2 \rightarrow NO_3^- + H^+ + O_2$	4.5(9)[b]	3.[b]	k_{A28}
(RA68)	$NO_3 + O_2^- \rightarrow NO_3^- + O_2$	1.(9)[b]	3.[b]	k_{A29}
(RA69)	$NO_3 + H_2O_2 \rightarrow NO_3^- + H^+ + HO_2$	1.(6)	5.5[b]	*Chameides* [1984]
(RA70)	$NO_3 + Cl^- \rightarrow NO_3^- + Cl$	1.(8)	3.[b]	*Ross and Neta* [1979]
(RA71)	$NO_3 + CH_3OH \xrightarrow{O_2} NO_3^- + H^+ + CH_2O + HO_2$	1.(6)[b]	5.5[b]	*Dogliotti and Hayon* [1967]
(RA72)	$NO_3 + HCOOH \xrightarrow{O_2} NO_3^- + H^+ + CO_2 + HO_2$	2.1(5)	6.4[b]	*Dogliotti and Hayon* [1967]
(RA73)	$NO_3 + HCOO^- \xrightarrow{O_2} NO_3^- + CO_2 + HO_2$	6.(7)[b]	3.[b]	see footnote[f]
	S(IV) Complexation and Oxidation			
(RA74)	$HSO_3^- + CH_2O \rightarrow HOCH_2SO_3^-$	7.9(2)	9.7[b]	*Boyce and Hoffmann* [1984]
(RA75)	$SO_3^{2-} + CH_2O \rightarrow HOCH_2SO_3^- + OH^-$	2.5(7)	3.6[b]	*Boyce and Hoffmann* [1984]
(RA76)	$HOCH_2SO_3^- + OH^- \rightarrow SO_3^{2-} + CH_2O + H_2O$	3.6(3)	9.[b]	*Munger et al.* [1986]
(RA77)	$HSO_3^- + OH \rightarrow SO_3^- + H_2O$	9.5(9)	3.[b]	*Adams and Boag* [1964]
(RA78)	$SO_3^{2-} + OH \rightarrow SO_3^- + OH^-$	5.5(9)	3.[b]	*Adams and Boag* [1964]
(RA79)	$HOCH_2SO_3^- + OH \rightarrow CH_2O + SO_3^- + H_2O$	1.4(9)[b]	3.[b]	see footnote[g]
(RA80)	$SO_3^- + O_2 \rightarrow SO_5^-$	1.5(9)	3.[b]	*Huie and Neta* [1984]
(RA81*a*)	$SO_5^- + HSO_3^- \rightarrow HSO_5^- + SO_3^-$	3.(6)	4.8[b]	*Huie and Neta* [1984][j]
(RA81*b*)[h]	$SO_5^- + HSO_3^- \rightarrow SO_4^- + SO_4^{2-} + H^+$			
(RA81*c*)[h]	$SO_5^- + HSO_3^- \rightarrow 2SO_4^{2-} + 2H^+ + OH$			
(RA82)	$SO_5^- + O_2^- \xrightarrow{H_2O} HSO_5^- + OH^- + O_2$	1.(8)[b]	3.[b]	k_{A22}
(RA83)	$SO_5^- + HCOOH \xrightarrow{O_2} HSO_5^- + CO_2 + HO_2$	2.(2)[b]	10.6[b]	see footnote[i]
(RA84)	$SO_5^- + HCOO^- \xrightarrow{O_2} HSO_5^- + CO_2 + O_2^-$	1.4(4)[b]	8.[b]	see footnote[i]
(RA85)	$SO_5^- + SO_5^- \rightarrow 2SO_4^- + O_2$	2.(8)[b]	3.[b]	see footnote[j]
(RA86)	$HSO_5^- + HSO_3^- + H^+ \rightarrow 2SO_4^{2-} + 3H^+$	7.5(7)[b]	9.45[b]	k_{A107}[k]
(RA87)	$HSO_5^- + OH \rightarrow SO_5^- + H_2O$	1.7(7)	3.8[b]	*Maruthamuthu and Neta* [1977]
(RA88)[d]	$HSO_5^- + SO_4^- \rightarrow SO_5^- + SO_4^{2-} + H^+$	$< 1.(5)$		*Maruthamuthu and Neta* [1977]
(RA89)[d]	$HSO_5^- + NO_2^- \rightarrow HSO_4^- + NO_3^-$	3.1(−1)	13.2	*Edwards and Mueller* [1962]
(RA90)[d]	$HSO_5^- + Cl^- \rightarrow SO_4^{2-} + HOCl$	1.8(−3)	14.0	*Fortnum et al.* [1960]
(RA91)	$SO_4^- + HSO_3^- \rightarrow SO_4^{2-} + H^+ + SO_3^-$	1.3(9)	3.[b]	*Hayon et al.* [1972]
(RA92)	$SO_4^- + SO_3^{2-} \rightarrow SO_4^{2-} + SO_3^-$	5.3(8)	3.[b]	*Hayon et al.* [1972]
(RA93)	$SO_4^- + HO_2 \rightarrow SO_4^{2-} + H^+ + O_2$	5.(9)[b]	3.[b]	see footnote[l]
(RA94)	$SO_4^- + O_2^- \rightarrow SO_4^{2-} + O_2$	5.(9)[b]	3.[b]	see footnote[l]
(RA95)	$SO_4^- + OH^- \rightarrow SO_4^{2-} + OH$	8.(7)	3.[b]	*Maruthamuthu and Neta* [1978]
(RA96)	$SO_4^- + H_2O_2 \rightarrow SO_4^{2-} + H^+ + HO_2$	1.2(7)	4.[b]	*Maruthamuthu and Neta* [1978]
(RA97)	$SO_4^- + NO_2^- \rightarrow SO_4^{2-} + NO_2$	8.8(8)	3.[b]	*Maruthamuthu and Neta* [1978]
(RA98)	$SO_4^- + CH_3OH \xrightarrow{O_2} SO_4^{2-} + H^+ + CH_2O + HO_2$	2.5(7)	3.6[b]	*Dogliotti and Hayon* [1967]
(RA99)	$SO_4^- + HCO_3^- \rightarrow SO_4^{2-} + H^+ + CO_3^-$	9.1(6)	4.2[b]	*Dogliotti and Hayon* [1967]
(RA100)	$SO_4^- + HCOO^- \xrightarrow{O_2} SO_4^{2-} + CO_2 + HO_2$	1.7(8)[b]	3.[b]	*Ross and Neta* [1979]
(RA101)	$SO_4^- + Cl^- \rightarrow SO_4^{2-} + Cl$	2.(8)	3.[b]	*Ross and Neta* [1979]
(RA102)	$SO_4^- + HCOOH \xrightarrow{O_2} SO_4^{2-} + H^+ + CO_2 + HO_2$	1.4(6)	5.3[b]	*Ross and Neta* [1979]
(RA103)	$HSO_3^- + Cl_2^- \rightarrow SO_3^- + H^+ + 2Cl^-$	4.6(7)	3.2[b]	see footnote[m]
(RA104)	$SO_3^{2-} + Cl_2^- \rightarrow SO_3^- + 2Cl^-$	2.3(7)	3.6[b]	see footnote[m]
(RA105)	$HSO_3^- + O_3 \rightarrow SO_4^{2-} + H^+ + O_2$	3.2(5)	9.6	*Hoffmann and Calvert* [1985]
(RA106)	$SO_3^{2-} + O_3 \rightarrow SO_4^{2-} + O_2$	1.(9)	8.	*Hoffmann and Calvert* [1985]
(RA107)	$HSO_3^- + H_2O_2 + H^+ \rightarrow SO_4^{2-} + 2H^+ + H_2O$	7.45(7)	9.45	*Hoffmann and Calvert* [1985]
(RA108)	$HSO_3^- + CH_3OOH + H^+ \rightarrow SO_4^{2-} + CH_3OH + 2H^+$	1.91(7)	7.56	J. A. Lind et al. (unpublished manuscript, 1986)

Rate constants are given at 298 K. Read 7.(9) as 7. × 10^9. Many reaction expressions in this table represent the sum of successive elementary reaction steps. The rate of the overall reaction is first-order in each of the species on the left-hand side of the reaction equation, to the exclusion of other species. Species above the reaction sign are reactants which do not enter into the rate expression, generally because they are involved in a non-rate-limiting step of the overall reaction.

$$\Phi_{in} = \frac{3\eta L D_{g,i}}{a^2} \langle n_i \rangle \quad (1)$$

and the volatilization flux Φ_{out} (in molecules per cubic centimeter of air per second) of species j to the gas phase is given by

$$\Phi_{out} = \frac{3\eta L D_{g,i}}{a^2} \frac{6.023 \times 10^{20} C_j^*}{K_H R T} \quad (2)$$

where a is the droplet radius, L is the liquid water content (vol/vol), $D_{g,i}$ is the diffusion coefficient of species i in air, $\langle n_i \rangle$ is the bulk gas-phase concentration (in molecules per cubic centimeter of air) far from the droplet surface, C_j^* is the aqueous-phase concentration (M) at the droplet surface, K_H is the Henry's law constant (M per atmosphere), $R = 8.314 \times 10^{-2}$ atm 1 mol^{-1} K^{-1} is the gas constant, T is the temperature, and η is a coefficient correcting for free molecular effects ($0 < \eta < 1$). The approximate expression for η proposed by *Fuchs and Sutugin* [1971] was adopted here:

$$\eta = \left\{1 + \left[\frac{1.33 + 0.71\, Kn^{-1}}{1 + Kn^{-1}} + \frac{4(1-\alpha)}{3\alpha}\right] Kn\right\}^{-1} \quad (3)$$

The Knudsen number Kn is the ratio of the mean free path of air to the droplet radius; the sticking coefficient α represents the probability that a gas molecule impinging on the droplet surface will stick to that surface. Figure 1 shows the dependence of η on α, for a range of cloud droplet radii.

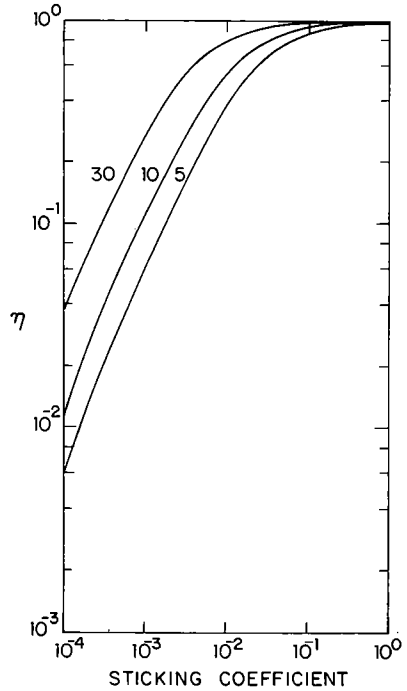

Fig. 1. Free molecular correction η to the continuum gas-droplet transfer flux, as a function of sticking coefficient, for droplet radii 5, 10, and 30 μm.

The sticking coefficient is a poorly known quantity, which appears to be quite specific to the nature of the impinging gas and the composition of the surface [*Chameides and Davis*, 1982]. If the droplet surface were coated by a film of organic surfactants, the surface resistance to gas-droplet transfer could be considerable [*Gill et al.*, 1983]. In the remote troposphere, however, the presence of such a film is unlikely because of the paucity of organic material; one would expect sticking coefficients larger than 10^{-4}, based on the sparse data available for the impingement of soluble gases on liquid water surfaces [*Schwartz*, 1986]. Further, one would expect α to increase with the solubility of the gas. An accurate estimate of α is important only for very soluble gases, which may take a long time to equilibrate between the gas phase and the aqueous phase; weakly soluble gases equilibrate on time scales of seconds or less, even if α is small [*Chameides*, 1984, 1985; *Jacob*, 1985]. Preliminary data from Aerodyne Research, Inc., and Boston College (M. A. Zahniser and P. Davidovits, personal communication, 1986) indicate that the sticking coefficients of very soluble gases on clean water surfaces range between 0.01 and 1. A value $\alpha = 0.1$ was chosen for the standard simulation; this value has the advantage of giving fairly accurate fluxes as long as α ranges between 0.05 and 1 (Figure 1). Sensitivity calculations will be conducted to evaluate the dependence of the chemistry on α.

Mathematical Formulation

The object of the calculations is to predict the chemical evolution of a well-mixed air parcel containing aqueous droplets. All droplets are assumed to have the same size and the same composition. A system of m chemical species is considered, which includes both gas-phase and aqueous-phase species. Two boundary conditions (Henry's law and flux matching) exist at the surface of the droplets between the concentrations of gas-phase and aqueous-phase species. These boundary conditions do not produce significant gradients in the concentrations of gas-phase species over the scale of the air parcel, because the fraction of the total air volume occupied by cloud droplets is small (10^{-7}–10^{-6}). Therefore if it

---

[a] The reaction ($HCO_3^- + O_2^-$) is not included, following the recommendation by *Schwartz* [1984].
[b] Estimated value.
[c] *Thomas and Ingold* [1968].
[d] Reaction not in the computational code.
[e] Estimated from (RA39) and the branching ratio of the gas-phase ($CH_3OOH + OH$) reaction.
[f] The relation $k_{A73} = k_{A72}\,(k_{A53}/k_{A52})$ is assumed.
[g] Estimated from the rate of reaction ($CH_3SO_3H + OH$) [*Lind and Eriksen*, 1975; *Saltzman et al.*, 1983].
[h] Branch (RA81*a*) is assumed in the standard simulations; sensitivity calculations are conducted with branches (RA81*b*) and (RA81*c*) (see text).
[i] Estimated from the rate of oxidation of ascorbic acid and ascorbate by SO_5^- [*Huie and Neta*, 1984], and a ratio of 10^4 between the rate constants for oxidation of formic acid (formate) and ascorbic acid (ascorbate) by CO_3^- and Cl_2^- [*Ross and Neta*, 1979].
[j] R. E. Huie, National Bureau of Standards, personal communication, 1985.
[k] See text for discussion.
[l] Assumed to be intermediate between the rates of $O_2(-I)$ oxidation by OH and Cl_2^-.
[m] Calculated from the reported rate of 3.3×10^7 M^{-1} s^{-1} for the reaction (Cl_2^- + S(IV)) at *p*H 7 [*Hagesawa and Neta*, 1978], assuming that HSO_3^- reacts twice as fast as SO_3^{2-} (as in the case of oxidation by OH).

is assumed that the air parcel is well mixed, it may also be assumed that the gas-phase species are well mixed within the air parcel.

Mass transport limitations within the cloud droplets must be examined carefully. The steady state diffusion equation for the concentration $C_j(r)$ (M) of aqueous-phase species j is

$$D_{aq,j}\frac{1}{r^2}\frac{d}{dr}\left(r^2\frac{dC_j}{dr}\right) - k_{L,j}(r)C_j + P_j(r) = 0 \qquad (4)$$

$$0 \le r \le a$$

where r is the distance from the center of the droplet, $D_{aq,j}$ is the aqueous-phase molecular diffusion coefficient, $k_{L,j}$ (per second) is the global first-order loss rate constant for species j, and P_j (M per second) is the global production rate of species j by aqueous-phase reactions. In (4) a family of aqueous-phase species is treated as a single species if the different species in the family are related to one another by equilibria established rapidly relative to the rate of other chemical reactions involving the individual species. For example, the S(IV) species $SO_2 \cdot H_2O$, HSO_3^-, and SO_3^{2-} are treated as a single species [see *Schwartz and Freiberg*, 1981]. Equation (4) is subject to the boundary conditions:

$$(dC_j/dr)_{r=0} = 0 \qquad (5)$$

$$C_j(a) = C_j^* \qquad (6)$$

On the basis of an aqueous-phase diffusion coefficient $D_{aq,j} = 2 \times 10^{-5}$ cm^2 s^{-1} (a typical value; [cf. *Schwartz*, 1986]), the characteristic time for diffusion within a 10-μm radius droplet is of order 5×10^{-3} s. Therefore an aqueous-phase species is well mixed within a 10-μm droplet if its lifetime against chemical removal ($k_{L,j}^{-1}$), and its characteristic time for aqueous-phase production (C_j/P_j), are both much longer than 5×10^{-3} s. Over the range of model simulations this condition is found to be verified for all species except O_3(aq), NO_3(aq), OH(aq), SO_4^-, CO_3^-, and Cl(aq) + Cl_2^-. Less reactive species are well mixed in the aqueous phase. The treatment of mass transport limitations in the cloud droplet chemistry can then be simplified considerably by noting that chemical reactions between the seven poorly mixed species do not contribute significantly to the chemical evolution of the system. These species are present at concentrations which are very low compared to the concentrations of the well-mixed species with which they react rapidly. Therefore the aqueous-phase reactions that need to be considered in the model are at most first order in the concentrations of poorly mixed species; the aqueous-phase reaction rates integrated over the droplet volume can be calculated directly from the bulk concentrations $\langle C_j \rangle$, defined by

$$\langle C_j \rangle = (\tfrac{4}{3}\pi a^3)^{-1}\int_0^a 4\pi r^2 C_j(r)\,dr \qquad (7)$$

The surface concentrations of O_3(aq), NO_3(aq), and OH(aq) must still be determined in order to calculate the volatilization fluxes of these species. The species O_3(aq) and NO_3(aq) are rapidly removed in the droplets by reactions with well-mixed species ($k_{L,j}$ independent of r), and they are not produced by aqueous-phase sources. The main contributors to $k_{L,j}$ are (RA27) and (RA106) for O_3(aq), and (RA69) and (RA70) for NO_3(aq). The solution to the aqueous-phase diffusion equation for O_3(aq) and NO_3(aq) is [*Schwartz and Freiberg*, 1981]

$$C_j(r) = C_j^*\frac{a}{r}\frac{\sinh(q_j r/a)}{\sinh q_j} \qquad 0 \le r \le a \qquad (8)$$

where

$$q_j = a\left(\frac{k_{L,j}}{D_{aq,j}}\right)^{1/2} \qquad (9)$$

By substituting (8) into (7), one can express the surface concentration C_j^* as a function of bulk concentrations:

$$C_j^* = \langle C_j \rangle\left[3\left(\frac{\coth q_j}{q_j} - \frac{1}{q_j^2}\right)\right]^{-1} \qquad (10)$$

The behavior of OH(aq) is more complicated than that of O_3(aq) or NO_3(aq). OH(aq) reacts rapidly with a number of well-mixed species (global first-order loss rate constant $k_{L,OH}$ independent of r) and is also produced within the aqueous phase. The main aqueous-phase source is the reaction O_2^- + O_3 (RA27); the rate of OH(aq) production by this reaction has a radial dependence which follows the radial dependence of the O_3(aq) concentration. The other OH(aq) sources (mainly (RA14)) involve only well-mixed species, and the corresponding OH(aq) production rates are independent of r. Let P_{OH}' represent the global rate of OH(aq) production by all aqueous-phase sources except (RA27) (P_{OH}' is independent of r):

$$P_{OH}(r) = P_{OH}' + k_{A27}\langle C_{O_2^-}\rangle C_{O_3}(r) \qquad (11)$$

The solution to the aqueous-phase diffusion equation for OH(aq) is

$$C_{OH}(r) = \frac{P_{OH}'}{k_{L,OH}} + \left(C_{OH}^* - \frac{P_{OH}'}{k_{L,OH}}\right)\frac{a}{r}\frac{\sinh(q_{OH}r/a)}{\sinh q_{OH}} + \frac{k_{A27}'\langle C_{O_2^-}\rangle C_{O_3}^*}{k_{L,OH} - k_{L,O_3}}\frac{a}{r}\left[\frac{\sinh(q_{O_3}r/a)}{\sinh q_{O_3}} - \frac{\sinh(q_{OH}r/a)}{\sinh q_{OH}}\right] \qquad (12)$$

By substituting (12) into (7), one can express the surface concentration $C_{OH}^*(a)$ as a function of bulk concentrations:

$$C_{OH}^* = \frac{P_{OH}'}{k_{L,OH}} + \frac{k_{A27}\langle C_{O_2^-}\rangle\langle C_{O_3}\rangle}{k_{L,OH} - k_{L,O_3}}\left[3\left(\frac{\coth q_{O_3}}{q_{O_3}} - \frac{1}{q_{O_3}^2}\right)\right]^{-1} + \left(\langle C_{OH}\rangle - \frac{P_{OH}'}{k_{L,OH}} - \frac{k_{A27}\langle C_{O_2^-}\rangle\langle C_{O_3}\rangle}{k_{L,OH} - k_{L,O_3}}\right) \cdot \left[3\left(\frac{\coth q_{OH}}{q_{OH}} - \frac{1}{q_{OH}^2}\right)\right]^{-1} \qquad (13)$$

Therefore the chemical system can be solved using bulk concentrations for all gas-phase and aqueous-phase species. No distinction is made in the mathematical treatment between these two types of species. Aqueous-phase concentrations and reaction rates are calculated in units of molecules per cubic centimeter of air, in the same way as gas-phase concentrations and reaction rates. Aqueous-phase reaction rate constants are scaled by the liquid water content of the cloud. The concentration $\langle n_j \rangle$ of aqueous-phase species j in molecules per cm^3 of air is obtained from $\langle C_j \rangle$ by:

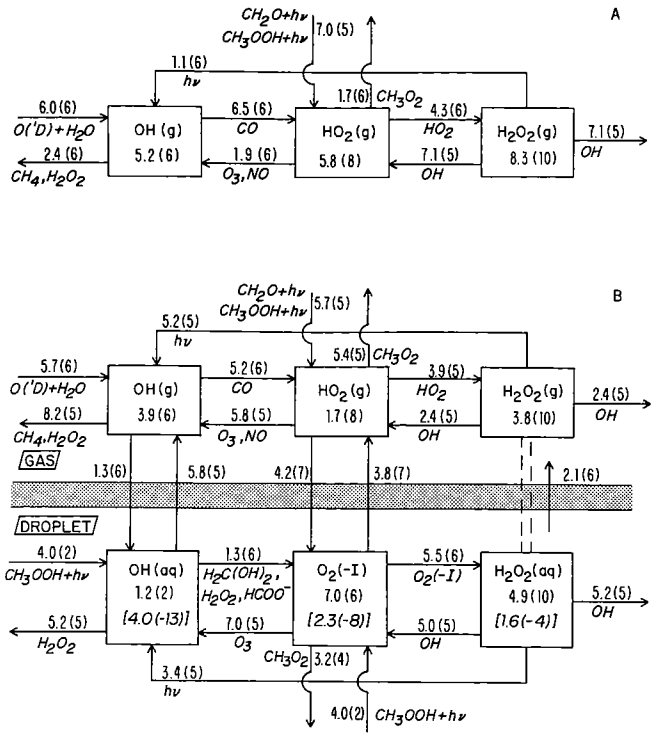

Fig. 2. The odd hydrogen cycle (*a*) immediately before cloud formation and (*b*) 1 hour after cloud formation. Model conditions are those of Table 1. The main reaction pathways are indicated. Concentrations are in units of molecules per cubic centimeter of air and transformation rates are in units of molecules odd H per cubic centimeter of air per second. Aqueous-phase concentrations (M) are given in brackets. The H_2O_2(aq) volatilization flux is given as the net flux; H_2O_2(g) and H_2O_2(aq) concentrations are within 1% of equilibrium by Henry's law.

$$\langle n_j \rangle = 6.023 \times 10^{20}\, L\, \langle C_j \rangle \qquad (14)$$

The evolution of the chemical composition of the air parcel is then determined by the system of m equations for gas-phase and aqueous-phase species:

$$\frac{d\langle n_k \rangle}{dt} = RP_k(\langle n_1 \rangle, \langle n_2 \rangle, \cdots, \langle n_m \rangle) - RL_k(\langle n_1 \rangle, \langle n_2 \rangle, \cdots, \langle n_m \rangle), \qquad (15)$$

where RP_k and RL_k are the total production and loss rates, respectively, of species k. These rates include gas-phase or aqueous-phase reaction rates, plus absorption and volatilization at the droplet surface. The reversible aqueous-phase reactions (RA1–RA12) are very fast [*Hoffmann*, 1981] and are constrained to be at equilibrium at all times in the calculations. The system of (15) is solved by an implicit finite difference method [*Richtmeyer*, 1957].

The Odd Hydrogen Cycle in Cloud

The standard simulation considers a cloud forming under the conditions of Table 1. The initial gas-phase composition of the air parcel is determined by iteration of the gas-phase chemical mechanism over successive diurnal cycles until identical noontime concentrations are reproduced from day to day. Figure 2*a* shows the gas-phase odd H cycle immediately before cloud formation, and Figure 2*b* shows the gas-phase and aqueous-phase odd H cycles one hour after cloud formation. Because OH has a very short lifetime and is involved in a large number of reactions, its chemistry is more complicated than that of the two other odd hydrogen species, H_2O_2 and HO_2. Therefore I will first discuss the in-cloud chemistry of H_2O_2 and HO_2 and from there discuss the chemistry of OH.

Hydrogen Peroxide

Hydrogen peroxide is very soluble in water, and a large fraction of H_2O_2(g) initially present is scavenged by the droplets upon cloud formation. In addition, H_2O_2(aq) is produced within the aqueous phase by recombination of perhydroxyl radicals. The rate of aqueous-phase H_2O_2(aq) production is enhanced considerably by partial dissociation of HO_2(aq) to O_2^-, because of rapid electron transfer between HO_2(aq) and O_2^-:

$$\text{(RA22)} \qquad HO_2 + O_2^- \xrightarrow{H_2O} H_2O_2 + O_2 + OH^-$$

In a cloud, aqueous-phase production of H_2O_2(aq) by (RA22) is much faster than production of H_2O_2(g) by the analogous gas-phase reaction $HO_2 + HO_2$ (Figure 2). Further, (RA22) is faster than gas-phase production of H_2O_2(g) in the initially clear atmosphere. Therefore H_2O_2 production is enhanced by the presence of cloud. The importance of aqueous-phase H_2O_2 production in clouds has been discussed by *Chameides* [1984].

Oxidation of S(IV) can be a very rapid sink for H_2O_2(aq) because the reaction

$$\text{(RA107)} \qquad HSO_3^- + H_2O_2 + H^+ \rightarrow SO_4^{2-} + 2H^+ + H_2O$$

is fast. In polluted environments where SO_2 is in excess of H_2O_2, (RA107) would deplete H_2O_2 from the atmosphere on a time scale of minutes [*Jacob and Hoffmann*, 1983; *Seigneur and Saxena*, 1984]. In the remote troposphere, however, H_2O_2 is in large excess of SO_2, so that the extent of H_2O_2 depletion by (RA107) is limited by the amount of SO_2 present. The present simulation assumes initial concentrations of 8.3×10^{10} molecules cm^{-3} air (3.4 ppb) and 2.5×10^9 molecules cm^{-3} air (0.1 ppb) for H_2O_2 and SO_2, respectively; under those conditions, (RA107) may remove at most 3% of the H_2O_2 initially present. After 1 hour of cloud, SO_2 has been nearly quantitatively oxidized and (RA107) has become a negligible sink for H_2O_2.

Hydrogen peroxide oxidizes other species in the aqueous phase besides S(IV), but all these reactions are very slow at atmospheric concentrations (Table 2*c*). The main chemical sinks for H_2O_2(aq), 1 hour after cloud formation, are photolysis and oxidation by OH(aq), both of which drive the aqueous-phase odd H cycle:

$$\text{(RA14)} \qquad H_2O_2 + h\nu \rightarrow 2OH$$

$$\text{(RA17)} \qquad OH + H_2O_2 \rightarrow H_2O + HO_2$$

Removal of H_2O_2(aq) by (RA14) and (RA17) is slower than aqueous-phase production of H_2O_2(aq) by (RA22). Therefore H_2O_2(aq) produced in the droplets is volatilized, and H_2O_2

TABLE 3. Sources and Sinks of OH(aq) in Cloud

Reaction No.	Reaction	Rate, $M\ s^{-1}$
	Sources	
(H2)	$OH(g) \rightarrow OH(aq)$	$2.5(-9)$
(RA14)	$H_2O_2 + h\nu \xrightarrow{H_2O} 2OH$	$(2x)\ 5.7(-10)$
(RA27)	$O_2^- + O_3 \rightarrow OH + 2O_2 + OH^-$	$2.3(-9)$
		$5.9(-9)^a$
	Sinks	
(RA44)	$OH + H_2C(OH)_2 \xrightarrow{O_2} HCOOH + HO_2 + H_2O$	$2.9(-9)$
(RA17)	$OH + H_2O_2 \rightarrow HO_2 + H_2O$	$1.7(-9)$
(RA47)	$OH + HCOO^- \xrightarrow{O_2} CO_2 + HO_2 + OH^-$	$1.2(-9)$
(RA19)	$OH + Cl^- + H^+ \rightarrow Cl + H_2O$	$2.1(-11)$
(RA15)	$OH + HO_2 \rightarrow O_2 + H_2O$	$4.8(-11)$
(RA46)	$OH + HCOOH \xrightarrow{O_2} CO_2 + HO_2 + H_2O$	$3.7(-11)$
(RA41)	$OH + CH_3OH \xrightarrow{O_2} CH_2O + HO_2 + H_2O$	$4.0(-11)$
(RA16)	$OH + O_2^- \rightarrow O_2 + OH^-$	$2.1(-11)$
		$5.9(-9)^b$

Read $2.5(-9)$ as 2.5×10^{-9}. Model conditions are those of Table 1, 1 hour after cloud formation (Figure 2*b*).

[a]Total rate for sources.

[b]Total rate for sinks.

accumulates in both the gas phase and the aqueous phase. The rate of H_2O_2 accumulation in both phases (1.8×10^6 molecules cm^{-3} air s^{-1}) is still fairly slow compared to the initial H_2O_2 concentration (8.3×10^{10} molecules cm^{-3} air), so that H_2O_2 concentrations are expected to show little change with time over the typical lifetime of a cloud. Concentrations of $H_2O_2(g)$ and $H_2O_2(aq)$ in cloud are mostly set by Henry's law partitioning of the initial H_2O_2 between the gas phase and the aqueous phase.

Perhydroxyl Radical

The perhydroxyl radical is very soluble in water, and its solubility is further enhanced by the acid-base dissociation of $HO_2(aq)$ ($pK_{298} = 4.69$):

$$\text{(RA2)} \qquad HO_2(aq) \rightleftarrows H^+ + O_2^- \qquad (16)$$

The species $HO_2(aq)$ and O_2^- are in rapid equilibrium in the aqueous phase, and it is convenient to define $O_2(-I)$ as their sum:

$$[O_2(-I)] = [HO_2(aq)] + [O_2^-]$$

In the aqueous phase, $O_2(-I)$ is rapidly removed by electron transfer reactions involving O_2^-:

$$\text{(RA27)} \qquad O_2^- + O_3 \xrightarrow{H_2O} OH + 2O_2 + OH^-$$

$$\text{(RA22)} \qquad HO_2 + O_2^- \xrightarrow{H_2O} H_2O_2 + O_2 + OH^-$$

If $HO_2(aq)$ did not dissociate (low *p*H), aqueous-phase removal of $O_2(-I)$ would proceed mostly by the reaction $HO_2 + HO_2$ (RA21), which is much slower than (RA22). Therefore the partial dissociation of $HO_2(aq)$ enhances the aqueous-phase removal of $O_2(-I)$, which in turn enhances the rate of scavenging of $HO_2(g)$ by the droplets. As a result, the fate of HO_2 in cloud is strongly dependent on the cloud water *p*H. This will be discussed in the next section.

In the standard simulation (*p*H = 4.16) the aqueous-phase reactions removing $O_2(-I)$ proceed sufficiently fast that equilibirum between $HO_2(g)$ and $HO_2(aq)$ is not fully achieved. Mass transport limitations involved in HO_2 gas-droplet transfer have been discussed in detail previously by *Schwartz* [1984]. Scavenging of $HO_2(g)$ from the gas phase constitutes the main source of $O_2(-I)$, but aqueous-phase oxidation of $H_2C(OH)_2$, $H_2O_2(aq)$, and $HCOO^-$ by OH(aq) provide important secondary sources of $O_2(-I)$:

$$\text{(RA44)} \quad H_2C(OH)_2 + OH \xrightarrow{O_2} HCOOH + HO_2 + H_2O$$

$$\text{(RA17)} \quad OH + H_2O_2 \rightarrow H_2O + HO_2$$

$$\text{(RA47)} \quad HCOO^- + OH \xrightarrow{O_2} CO_2 + HO_2 + OH^-$$

Because of the rapid aqueous-phase removal of O_2^- the droplets constitute a dynamic sink for $HO_2(g)$ which is much more rapid than the gas-phase $HO_2(g)$ sinks. As a result, $HO_2(g)$ is depleted in the cloud; the concentration of $HO_2(g)$ in the cloud is only 29% of the concentration before cloud formation. The scavenging of $HO_2(g)$ interrupts the gas-phase odd H cycle by slowing down the conversions $HO_2(g) \rightarrow OH(g)$ and $HO_2(g) \rightarrow H_2O_2(g)$, and instead, drives the aqueous-phase odd H cycle by the conversions $O_2(-I) \rightarrow OH(aq)$ and $O_2(-I) \rightarrow H_2O_2(aq)$ (reactions (RA27) and (RA22)). We have previously seen that this modification of the odd H cycle leads to enhanced production of H_2O_2 in clouds but has only minor implications on the H_2O_2 concentration; as we will now see, the effect on OH chemistry is considerably more important.

Hydroxyl Radical

The OH radical is less soluble than H_2O_2 or HO_2 (Table 2). However, Figure 2 shows that the concentrations of OH(g) and OH(aq) are controlled more by homogeneous sources and sinks than by exchanges at the droplet surface. Therefore the coupling by gas-droplet transfer between gas-phase and aqueous-phase OH concentrations is less important than in the case of H_2O_2 or HO_2.

The concentration of OH(g) in cloud is 25% lower than the concentration before cloud formation. Gas-phase production of OH(g) is slowed down in the cloud because of the depletion of $HO_2(g)$ and $H_2O_2(g)$. On the other hand, the gas-phase sinks are little affected by cloud because CO and CH_4, the main species removing OH(g), are not scavenged by the cloud droplets. Loss of OH(g) by transfer to the aqueous phase is slower than the gas-phase OH(g) sinks and has only a minor effect on OH(g) concentrations. Therefore the main cause of the decrease of OH(g) concentrations in cloud is not the scavenging of OH(g) but rather the scavenging of $H_2O_2(g)$ and $HO_2(g)$.

Table 3 lists the main sources and sinks of OH(aq) and their rates. The species $H_2O_2(aq)$ and $O_2(-I)$ are important sources of OH(aq) by (RA14) and (RA27). Scavenging of OH(g) provides a source of OH(aq) which is of comparable importance to these two aqueous-phase sources. The main OH(aq) sinks are the oxidation reactions with $H_2C(OH)_2$, $H_2O_2(aq)$, and $HCOO^-$, three of the most abundant reduced species.

From Table 3 the chemical lifetime of OH(aq) is 6.7×10^{-5} s. Because of this short lifetime, OH(aq) is poorly mixed within

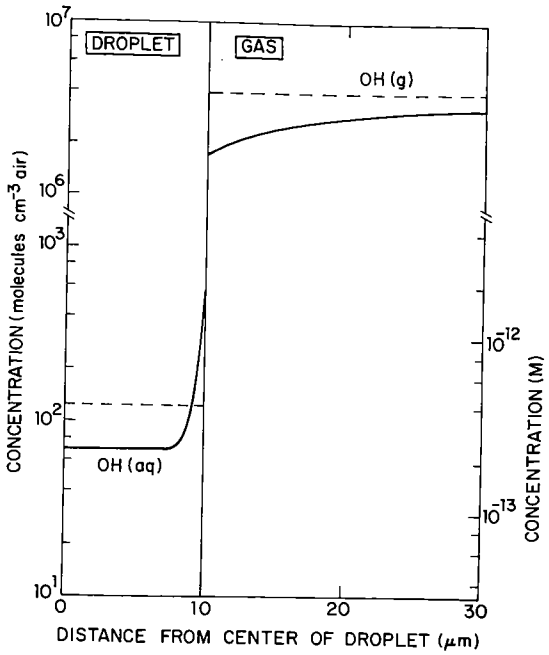

Fig. 3. Concentrations of OH(aq) and OH(g) as a function of distance from the center of a droplet, 1 hour after cloud formation. Dashed lines represent bulk concentrations in each phase. Model conditions are those of Table 1.

the droplets (Figure 3). The OH(aq) concentration away from the droplet surface is not affected by gas-droplet transfer; OH(g) absorbed at the surface of the droplet reacts before it can penetrate to the interior of the droplet, while OH(aq) produced in the droplet interior by aqueous-phase reactions is reduced before it can be volatilized at the droplet surface. Therefore the concentration of OH(aq) in the droplet interior approaches an aqueous-phase chemical steady state value given by a balance between aqueous-phase sources and sinks, excluding gas-droplet transfer. From Table 3, the aqueous-phase production rate of OH(aq) is 3.4×10^{-9} M s^{-1}, and the aqueous-phase first-order loss rate constant is 1.5×10^{4} s^{-1}, so that the aqueous-phase chemical steady state OH(aq) concentration in the droplet interior is 2.3×10^{-13} M. The surface concentration of OH(aq) is 1.8×10^{-12} M, 4.4 times higher than the bulk concentration (4.0×10^{13} M).

Because of the high surface concentration of OH(aq) the rate of transfer of OH(g) to the aqueous phase is slower than it would be if OH(aq) were well mixed in the droplets. The sensitivity of the overall chemistry to the poor mixing of short-lived species was examined by conducting the same simulation as above but with O_3(aq), NO_3(aq), and OH(aq) assumed to be well mixed in the droplets. That simulation gave OH(aq) concentrations 21% too high and OH(g) concentrations 5% too low. The concentrations of HCOOH and HSO_5^- were 11% and 18% too high, respectively. None of the other species were affected by more than 10%. Therefore the poor mixing of short-lived aqueous-phase species does not appear to be a major factor in the overall chemistry of a remote cloud.

The Methane Oxidation Chain and The Production of Formic Acid

Methane is converted to CO_2 in the gas phase by a series of successive oxidation steps involving OH(g) [*Logan et al.*, 1981]. Figure 4*a* shows the CH_4 oxidation chain in the clear atmosphere preceding the cloud, with the standard model conditions (Table 1). Cloud formation perturbs the CH_4 oxidation chain by scavenging of water-soluble intermediates (CH_3O_2, CH_3OOH, CH_2O, HCOOH). A parallel oxidation chain is set up in the aqueous phase as these scavenged intermediates react with aqueous-phase odd H species.

Figure 4*b* shows the CH_4 oxidation chain 1 hour after cloud formation. The initial attack of OH(g) on CH_4 to produce CH_3O_2 is slower than before cloud formation because of the lower OH(g) concentration. The gas-phase reaction of CH_3O_2(g) with NO(g) to produce CH_2O(g) is not inhibited by cloud formation because of the low solubility of NO; on the other hand, the gas-phase reaction of CH_3O_2(g) with HO_2(g) to produce CH_3OOH(g) is inhibited because of the depletion of HO_2(g). The Henry's law constant for CH_3O_2 is estimated to be of order unity (Table 2*a*), so that the droplets do not constitute a significant CH_3O_2 sink. In the aqueous phase, CH_3O_2(aq) should react rapidly with O_2^- to produce CH_3OOH(aq):

$$\text{(RA37)} \quad CH_3O_2 + O_2^- \xrightarrow{H_2O} CH_3OOH + O_2 + OH^-$$

The main sink for CH_3OOH(aq) is volatilization to the gas phase, where it may cycle back to CH_3O_2(g) or be converted to CH_2O(g). Oxidation of HSO_3^- by CH_3OOH(aq) is unimportant past the first few minutes of cloud, because of the total depletion of SO_2.

The aqueous phase is not a significant source of CH_2O; oxidation of CH_3OOH(aq) and CH_3OH(aq) contribute less than 1% of the total CH_2O produced in cloud. On the other hand, cloud droplets provide an important sink for CH_2O produced in the gas phase. Formaldehyde is very soluble in water because it hydrates to its diol form, methylene glycol:

$$\text{(RA10)} \quad CH_2O \overset{H_2O}{\rightleftarrows} H_2C(OH)_2$$

The equilibrium constant for (RA10) is 1.8×10^3, so that CH_2O in cloud water is almost totally present as $H_2C(OH)_2$. Methylene glycol does not photolyze but is rapidly oxidized by OH(aq) to produce HCOOH via (RA44). Therefore cloud formation introduces an important CH_2O sink as $H_2C(OH)_2$ oxidized by OH(aq) is replenished by scavenging of CH_2O(g). This droplet sink results in the slow depletion of CH_2O in cloud, on a time scale of several hours.

Aqueous-phase production of HCOOH by the reaction $H_2C(OH)_2$ + OH is 3 orders of magnitude faster than gas-phase production. Over the first few minutes of cloud, this aqueous-phase source produces more HCOOH than was initially present in the gas phase. Therefore the HCOOH concentration in cloud becomes rapidly independent of the initial amount of atmospheric HCOOH. Under cloud-free conditions the lifetime of HCOOH against oxidation by OH(g) is several weeks; depending on the frequency of clouds and rain at a given location, one may expect clouds to control the atmospheric concentration of HCOOH. The importance of clouds as a source of HCOOH has been pointed out previously by *Chameides* [1984] and *Adewuyi et al.* [1984].

Clouds are not only a rapid source of HCOOH but also a rapid sink. The aqueous-phase sink ($HCOO^-$ + OH) is 3 orders of magnitude faster than the gas-phase sink (HCOOH + OH). Therefore the cloud is not an efficient source of HCOOH if the HCOOH produced remains in the

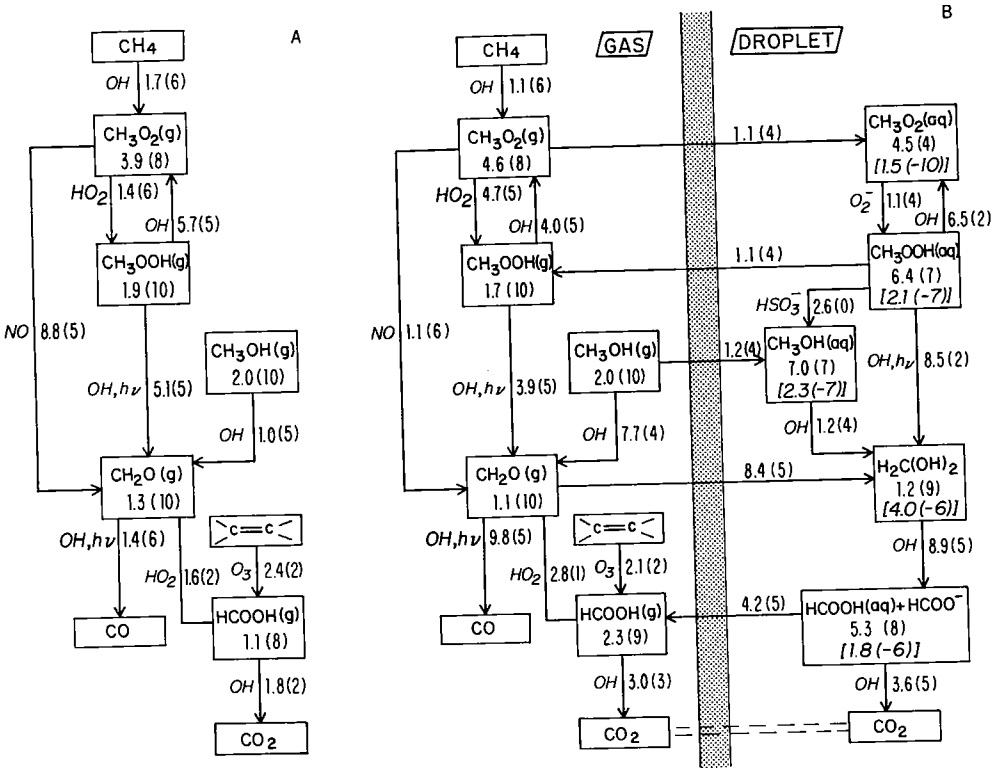

Fig. 4. The methane oxidation chain (*a*) immediately before cloud formation and (*b*) 1 hour after cloud formation. Model conditions are those of Table 1. The main reaction pathways are indicated. Concentrations are in units of molecules per cubic centimeter of air and transformation rates are in units of molecules per cubic centimeter of air per second. Aqueous-phase concentrations (M) are given in brackets. Gas-droplet transfer rates are given as net fluxes; all species are within 1% of equilibrium by Henry's law.

aqueous phase. Formic acid produced in the aqueous phase can be stabilized by volatilizing to the gas phase, where it has a long lifetime against oxidation by OH(g). The volatilization of HCOOH depends on the degree of HCOOH(aq)/$HCOO^-$ dissociation in the droplet ($pK_{298} = 3.75$) and is thus strongly pH dependent. In the standard simulation shown in Figure 4, most of the HCOOH produced in the droplets volatilizes; after 1 hour of cloud, HCOOH has accumulated in the gas phase to 2.3×10^9 molecules cm^{-3} (0.09 ppb). The cloud water pH in this simulation is low (pH = 4.16), which facilitates the volatilization of HCOOH and its subsequent accumulation. At higher pH, accumulation of HCOOH would be much less efficient, as is discussed later.

The value of the Henry's Law constant for HCOOH is uncertain at this date. In the model, $K_{H9} = 3.7 \times 10^3$ M atm^{-1} at 298 K is used, which was calculated from free energy data for HCOOH(g) and HCOOH(aq) compiled by *Latimer* [1952]. Two more recent compilations give slightly different values for the free energies of formation of HCOOH(g) [*Chao and Zwolinski*, 1978] and HCOOH(aq) [*Wagman et al.*, 1982]. From these data one calculates $K_{H9} = 5.6 \times 10^3$ M atm^{-1}. This discrepancy appears to be within the uncertainties on the free energy data. The sensitivity of the model results to the value selected for K_{H9} was tested by running a simulation with standard conditions (Table 1), but with $K_{H9} = 5.6 \times 10^3$ M atm^{-1}. Concentrations of HCOOH(g) and $HCOO^-$ 1 hour after cloud formation were 18% lower and 23% higher than in the standard simulation, respectively. Concentrations of all other species differed by less than 5%. Therefore the model results show little sensitivity to the uncertainty on K_{H9}.

Oxidation of S(IV) by OH(aq)

Sulfur dioxide is absorbed by cloud droplets and dissociates in the aqueous phase:

(H16) $$SO_2(g) \overset{H_2O}{\rightleftarrows} SO_2 \cdot H_2O$$

(RA7) $$SO_2 \cdot H_2O \rightleftarrows H^+ + HSO_3^-$$

(RA8) $$HSO_3^- \rightleftarrows H^+ + SO_3^{2-}$$

Oxidation of HSO_3^- and SO_3^{2-} by OH(aq) produces the SO_3^- radical [*Dogliotti and Hayon*, 1968]:

(RA77) $$HSO_3^- + OH \rightarrow SO_3^- + H_2O$$

(RA78) $$SO_3^{2-} + OH \rightarrow SO_3^- + OH^-$$

Under atmospheric conditions, SO_3^- rapidly adds O_2 [*Huie and Neta*, 1984]:

(RA80) $$SO_3^- + O_2 \rightarrow SO_5^-$$

The radical SO_5^- is a mild oxidant (E (SO_5^-/HSO_5^-) = 1.1 V; *Huie and Neta*, [1984]). *McElroy* [1986] has suggested that SO_5^- would rapidly oxidize Cl^-, but this reaction does not appear to be thermodynamically favorable. Instead, I expect the main sinks for SO_5^- in a remote cloud to be the exothermic reactions with O_2^-, $HCOO^-$, and HSO_3^-:

(RA82) $$SO_5^- + O_2^- \overset{H_2O}{\rightarrow} HSO_5^- + OH^- + O_2$$

(RA84) $$SO_5^- + HCOO^- \overset{O_2}{\rightarrow} HSO_5^- + CO_2 + O_2^-$$

(RA81*a*) $SO_5^- + HSO_3^- \rightarrow HSO_5^- + SO_3^-$

(RA81*b*) $SO_5^- + HSO_3^- \rightarrow SO_4^- + SO_4^{2-} + H^+$

(RA81*c*) $SO_5^- + HSO_3^- \xrightarrow{H_2O} 2SO_4^{2-} + 2H^+ + OH$

Caro's acid, H_2SO_5, is produced by (RA82) and (RA84), and by (RA81*a*). The first and second *p*Ks for H_2SO_5 are <2 and 10, respectively [*Kyrki*, 1963]; at the *p*H values found in cloud, the species present is HSO_5^- (peroxymonosulfate). Peroxymonosulfate is a strong oxidant (E (HSO_5^-/HSO_4^-) = 1.82 V; *Steele and Appelman* [1982]). Hydrogen peroxide has a similar redox potential (E (H_2O_2/H_2O) = 1.77 V; *Latimer* [1952]). The chemical properties of HSO_5^- should follow those of H_2O_2(aq), so I expect the main sinks to be reduction of OH(aq) and oxidation of HSO_3^-:

(RA87) $HSO_5^- + OH \rightarrow SO_5^- + H_2O$

(RA86) $HSO_5^- + HSO_3^- \rightarrow 2SO_4^{2-} + 2H^+$

Peroxymonosulfate also oxidizes Cl^- [*Fortnum et al.*, 1962] and NO_2^- [*Edwards and Mueller*, 1962] by nucleophilic displacement on oxygen, but these reactions are slow at atmospheric concentrations. Decomposition by self-reaction ($HSO_5^- + SO_5^{2-}$) is very slow at atmospheric concentrations [*Edwards*, 1964]. Oxidation of HSO_5^- by OH(aq) proceeds with a rate constant similar to that for the oxidation of H_2O_2(aq) [*Maruthamuthu and Neta*, 1977].

No kinetic data are available for the oxidation of S(IV) by HSO_5^-. *Devuyst et al.* [1979] have reported that the oxidation by air of a Na_2SO_3 solution at *p*H > 8 yields significant concentrations of a stable oxidant with the properties of HSO_5^-; the yield of this oxidant is zero below *p*H 8 and increases with *p*H above *p*H 8. This result suggests that the oxidation of S(IV) by HSO_5^- is an acid-catalyzed reaction, similar to oxidation by other peroxides such as H_2O_2(aq) or CH_3OOH(aq) (J. A. Lind et al., unpublished manuscript, 1986). In the present mechanism it is assumed that the rate law for (RA86) is the same as that for the oxidation of S(IV) by H_2O_2(aq).

The branching ratio (RA81*a*):(RA81*b*):(RA81*c*) is uncertain at this date. The results of *Devuyst et al.* [1979] suggest that the pathway (RA81*a*) is important. Pathway (RA81*a*) propagates a chain reaction in which HSO_3^- is oxidized to HSO_5^- by the addition of O_2(aq). Pathway (RA81*b*) produces SO_4^-, which can also propagate the S(IV) oxidation chain by reacting with HSO_3^-, following (RA91). However, SO_4^- is a very strong oxidant [*Maruthamuthu and Neta*, 1978] and is more likely to terminate the chain by oxidation of species more abundant than HSO_3^-, in particular, Cl^- [*McElroy*, 1986]. Therefore pathway (RA81*a*) is a more effective propagation step than (RA81*b*).

More generally, the efficiency with which the S(IV) oxidation chain is propagated is determined by the relative abundances of S(IV) on the one hand and other oxidizable species on the other hand. In the remote troposphere, S(IV) constitutes only a small fraction of total oxidizable material and is rapidly depleted by H_2O_2. The species $H_2C(OH)_2$, $HCOO^-$, Cl^-, and H_2O_2(aq) are all more abundant than S(IV) and compete for oxidation by SO_4^-. The species O_2^- and $HCOO^-$ compete with S(IV) for oxidation by SO_5^-. Therefore little chain propagation is expected. In polluted environments, however, S(IV) is one of the most abundant oxidizable species and is present in excess of H_2O_2. Under such conditions, oxidation of S(IV) by OH(aq) may be very efficient at producing HSO_5^- and SO_4^{2-}, even under acidic conditions, because of the propagation of the oxidation chain.

The role of OH(aq) in the oxidation of S(IV) is particularly important when S(IV) is present as a S(IV)-CH_2O adduct, hydroxymethanesulfonate (HMSA). Above *p*H 3, HMSA is mostly produced by the reaction of SO_3^{2-} with nonhydrated CH_2O(aq) [*Boyce and Hoffmann*, 1984]:

(RA75) $SO_3^{2-} + CH_2O \xrightarrow{H_2O} HOCH_2SO_3^- + OH^-$

Recent kinetic studies [*Kok et al.*, 1986; *Deister et al.*, 1986] suggest that dissociation of HMSA proceeds by nucleophilic displacement of HSO_3^- by OH^- [*Munger et al.*, 1986]:

(RA76) $HOCH_2SO_3^- + OH^- \rightarrow CH_2O + SO_3^{2-} + H_2O$

This dissociation reaction is rapid under alkaline conditions but is very slow at the *p*H values found in cloud; the lifetime of HMSA against dissociation is of the order of 100 hours at *p*H 5. The formation of HMSA is of particular interest, because HMSA is not oxidized by H_2O_2(aq) [*Kok et al.*, 1986] or O_3(aq) [*Hoigne et al.*, 1985]. Therefore formation of HMSA could stabilize S(IV) in the cloud and has been invoked to explain the observation of high S(IV) concentrations in nighttime fogs [*Munger et al.*, 1984]. However, HMSA is likely to be rapidly oxidized by OH(aq) in the daytime. M. R. Hoffmann (California Institute of Technology, private communication, 1986) has observed an explosive reaction upon addition of Fe^{2+} to a solution containing HMSA and H_2O_2(aq), probably due to the decomposition of H_2O_2(aq) to OH(aq) [*Walling*, 1975], followed by OH(aq) attack on HMSA. The oxidation reaction

(RA79) $HOCH_2SO_3^- + OH \rightarrow CH_2O + SO_3^- + H_2O$

initiates the reaction chain discussed above. Based on the bulk OH(aq) concentration of 4.0×10^{-13} M in the standard simulation and an estimated rate constant of 1.4×10^9 M^- s^{-1} for (RA79), the lifetime of HMSA in cloud is expected to be of the order of 30 min. Therefore HMSA should be efficiently oxidized by OH(aq) in clouds under noontime radiation conditions.

SIMULATIONS OVER A RANGE OF CLOUD WATER *p*H

Odd Hydrogen

The *p*K of the HO_2(aq)/O_2^- couple is 4.69, which is in the range of *p*H values found in atmospheric cloud water. Therefore the concentrations of odd H species are expected to be strongly *p*H dependent. The sensitivity to *p*H is explored here by a series of simulations using the model conditions of Table 1 but with condensation nuclei of various acidities.

Figure 5 shows the dependence of the concentrations of OH and HO_2 species on cloud water *p*H, 1 hour after cloud formation. The concentration of OH(g) shows little sensitivity to *p*H because the main source, the reaction $O(^1D) + H_2O$, and the main sinks, the reactions OH + CO and OH + CH_4, do not involve HO_2. The reaction OH + CO is in turn the main source of HO_2(g), so that HO_2(g) production shows little dependence on *p*H. However, loss of HO_2(g) by transfer to the droplets increases with increasing *p*H, because it is driven by the removal of O_2^- in the aqueous phase. Therefore a steady decrease in HO_2(g) concentration is found as the *p*H rises from 3 to 6. Above *p*H 6 the dependence of the HO_2(g) concentration on *p*H becomes progressively weaker; O_2(−I) is

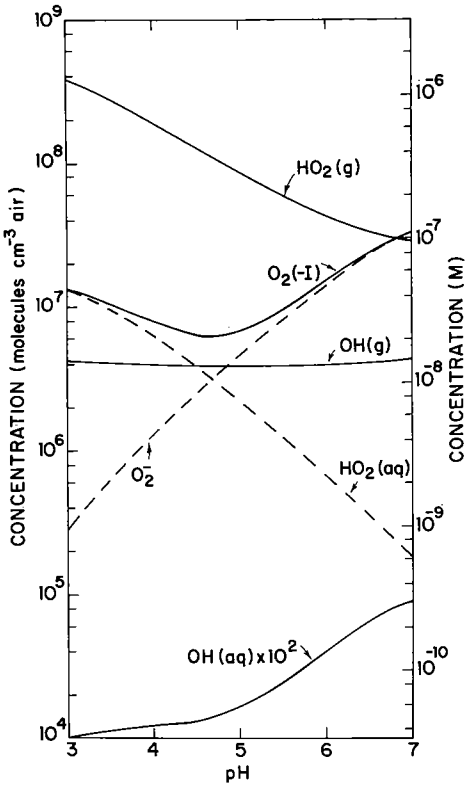

Fig. 5. Concentrations of odd hydrogen species 1 hour after cloud formation, as a function of cloud water *p*H. Model conditions are those of Table 1. Gas-phase concentrations are in units of molecules per cubic centimeter of air (left-hand scale), and aqueous-phase concentrations are in units of moles per liter of water (right-hand scale). Both scales are equivalent (equation (14)).

then nearly entirely dissociated, so that the droplets behave essentially as a diffusion-limited sink for HO_2(g).

The concentration of $O_2(-I)$ decreases with increasing *p*H up to pK_{HO_2}. Most of the $O_2(-I)$ in that low *p*H range is present as HO_2(aq), so that loss of $O_2(-I)$ by aqueous-phase reactions is slow. Under those conditions, HO_2(aq) approaches Henry's law equilibrium with HO_2(g), and the dependence of $O_2(-I)$ on *p*H follows that of HO_2(g). At *p*H values above pK_{HO_2}, however, the flux of HO_2(g) to the droplets is considerably enhanced by the dissociation of HO_2(aq) to O_2^-, so that the $O_2(-I)$ concentration increases with increasing *p*H. The concentration of $O_2(-I)$ goes through a minimum at *p*H $\approx pK_{HO_2}$. The dependence of the $O_2(-I)$ concentration on *p*H becomes progressively weaker above *p*H 6, as $O_2(-I)$ then approaches a steady state between production by diffusion-limited scavenging of HO_2(g) and loss by the reaction $O_2^- + O_3$.

The concentration of OH(aq) increases with increasing *p*H because of the increase in O_2^- concentration, which enhances the rate of OH(aq) production by the reaction $O_2^- + O_3$. The dependence of the OH(aq) concentration on *p*H becomes weaker above *p*H 6, following the pattern of the O_2^- concentration. At high *p*H the reaction $O_2^- + O_3$ is so rapid that OH(aq) is supersaturated in the droplet and volatilizes to the gas phase. The aqueous phase is then a source of OH(g); this explains the slight increase in the OH(g) concentration at high *p*H.

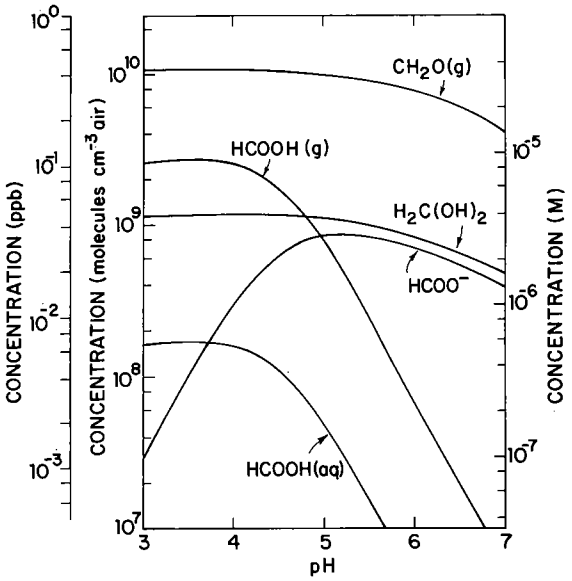

Fig. 6. Concentrations of CH_2O and HCOOH species 1 hour after cloud formation, as a function of cloud water *p*H. Model conditions are those of Table 1. Gas-phase concentrations are in units of molecules per cubic centimeter of air and ppb (left-hand scales), and aqueous-phase concentrations are in units of moles per liter of water (right-hand scale). The scales are equivalent (equation (14)).

Formic Acid

Figure 6 shows the concentrations of CH_2O and HCOOH species 1 hour after cloud formation, as a function of cloud water *p*H. As the *p*H increases and the OH(aq) concentration increases, the aqueous-phase HCOOH source, reaction $H_2C(OH)_2$ + OH, also rises. At low *p*H most of the HCOOH produced in the aqueous phase volatilizes to the gas phase, where it has a long lifetime against oxidation by OH(g). As the *p*H increases, however, an increasing fraction of the HCOOH produced remains in the aqueous phase as $HCOO^-$ and is

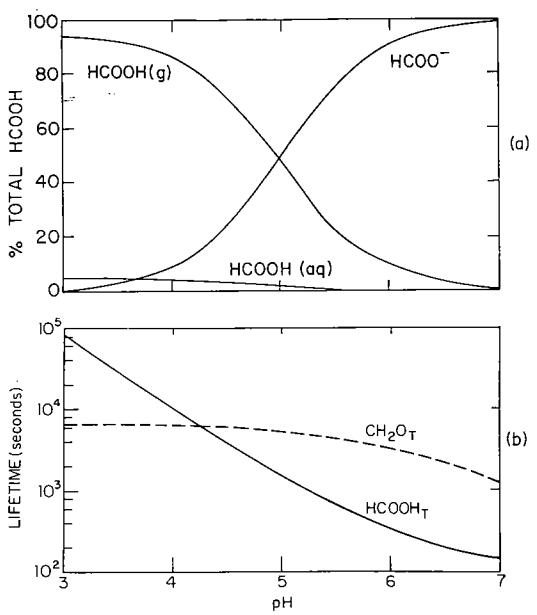

Fig. 7. (*a*) Equilibrium speciation of HCOOH in the cloud and (*b*) chemical lifetimes of $HCOOH_T$ (=HCOOH(g) + HCOOH(aq) + $HCOO^-$) and CH_2O_T (=CH_2O(g) + $H_2C(OH)_2$). Model conditions are those of Table 1.

oxidized by the rapid reaction $HCOO^- + OH$. A maximum in the total (gas phase plus aqueous phase) HCOOH concentration is found at $pH \approx 3.5$; at that pH, HCOOH is mostly in the gas phase. The total HCOOH concentration decreases rapidly with increasing pH above pH 4. A maximum in the aqueous-phase $HCOO^-$ concentration is found at $pH \approx 5$.

The dependence of the concentrations of HCOOH species on pH can be clearly explained with simple thermodynamic and kinetic arguments. The characteristic time for HCOOH to equilibrate between the gas phase and the aqueous phase is less than 1 min for $pH < 7$ [*Chameides*, 1985]; the oxidation of $HCOO^-$ is slower, even at high pH. Therefore the species HCOOH(g), HCOOH(aq), and $HCOO^-$ are at equilibrium. The fractions x, y, z, of HCOOH present as HCOOH(g), HCOOH(aq), and $HCOO^-$, respectively, are given by

$$x = \frac{1}{RT\beta} \tag{17a}$$

$$y = \frac{LK_{H9}}{\beta} \tag{17b}$$

$$z = \frac{LK_{H9}K_{A4}}{\beta[H^+]} \tag{17c}$$

$$\beta = \frac{1}{RT} + LK_{H9}\left(1 + \frac{K_{A4}}{[H^+]}\right) \tag{17d}$$

Figure 7*a* shows the equilibrium speciation of HCOOH, as a function of pH. Let $HCOOH_T$ represent total (gas phase plus aqueous phase) HCOOH:

$$n_{HCOOH_T} = n_{HCOOH(g)} + 6.023 \times 10^{20}\, L\{[HCOOH(aq)] + [HCOO^-]\} \tag{18}$$

The chemical lifetime of $HCOOH_T$ in cloud, τ_{HCOOH_T}, is given by

$$\tau_{HCOOH_T} = \{xk_{G13}n_{OH(g)} + (yk_{A46} + zk_{A47})[OH(aq)]\}^{-1} \tag{19}$$

This lifetime ranges over almost 2 orders of magnitude between pH 3 and pH 7 (Figure 7*b*). Above pH 3.5, τ_{HCOOH_T} is given to a good approximation by the lifetime of $HCOO^-$, that is, loss of HCOOH in the atmosphere is controlled by the aqueous-phase reaction $HCOO^- + OH$:

$$\tau_{HCOOH_T} \approx \{zk_{A47}[OH(aq)]\}^{-1} \tag{20}$$

Chameides [1984] has argued that a steady state in cloud is approached between production of HCOOH by the aqueous-phase source $H_2C(OH)_2 + OH$ and depletion by the aqueous-phase sink $HCOO^- + OH$, so that:

$$\frac{[HCOO^-]}{[H_2C(OH)_2]} = \frac{k_{A44}}{k_{A47}} \tag{21}$$

The present calculation indicates that (21) is a correct steady state representation for cloud water pH values above 3.5. The characteristic time for reaching this constant ratio between $HCOO^-$ and $H_2C(OH)_2$ concentrations is given by τ_{HCOOH_T} and ranges from 2 min at pH 7 to 8 hours at pH 3.5 (Figure 7*b*). Note, however, that the characteristic time for the concentration of HCOOH to approach a steady state is dependent on the time required for the $H_2C(OH)_2$ concentration to itself approach steady state. Figure 7*b* shows the chemical lifetime $\tau_{CH_2O_T}$ of total CH_2O in cloud (CH_2O(g) + $H_2C(OH)_2$), calculated in the same manner as τ_{HCOOH_T}.

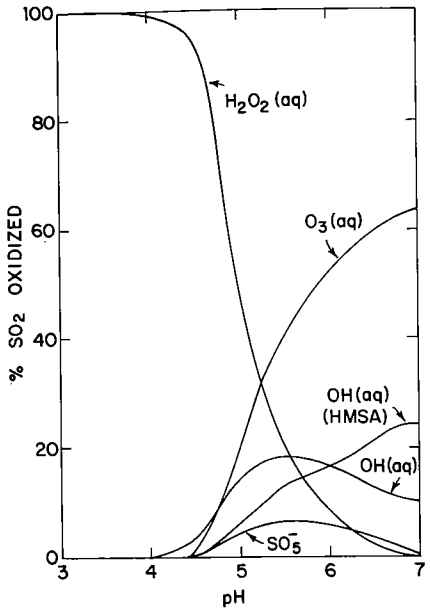

Fig. 8. Contributions of individual aqueous-phase oxidants to the oxidation of SO_2, as a function of cloud water pH. The label OH (HMSA) indicates the oxidation of HMSA by OH(aq). Model conditions are those of Table 1.

Above pH 4.2, $\tau_{CH_2O_T} > \tau_{HCOOH_T}$, so the attainment of a steady state for the concentration of HCOOH is controlled by $\tau_{CH_2O_T}$. Therefore even at high pH, it takes on the order of 1 hour for HCOOH to approach a steady state concentration in cloud.

In Figure 6 the steady state ratio (21) between $H_2C(OH)_2$ and $HCOO^-$ concentrations, as shown by parallel curves in the concentration versus pH profiles, is verified only for $pH > 5$. At lower pH most of the HCOOH produced in the aqueous phase is volatilized (Figure 7*a*), and several hours are required to accumulate sufficient amounts of $HCOO^-$ to balance the $H_2C(OH)_2 + OH$ source. This explains the maximum in the $HCOO^-$ concentration observed at $pH \approx 5$. One also notes that the dependence of the HCOOH(g) concentration on pH becomes very weak below pH 4; this is because removal of HCOOH is too slow to be a significant HCOOH sink during the first hour of cloud. Below pH 3.5 the HCOOH(g) concentration increases with increasing pH because the OH(aq) concentration increases, and therefore the rate of HCOOH production increases. This explains the maximum in the HCOOH(g) concentration at $pH \approx 3.5$.

Data for $HCOO^-$ concentrations in precipitation at remote marine sites have been collected by W. C. Keene and J. N. Galloway from the University of Virginia (private communication, 1986). They report volume-weighted average $HCOO^-$ concentrations ranging from 1.4 to 4.2 μeq l^{-1} for three different sites, with rainwater pH values typically close to 5. The cloud water $HCOO^-$ concentration predicted by the present model at pH 5 is 2.4 μeq L^{-1}, which is in the range of the observed rainwater concentrations. Therefore the model results are consistent with the currently available field data.

S(IV) Oxidation

Complete oxidation of S(IV) proceeds rapidly in a remote cloud because oxidants are present in large excess of SO_2. After 1 hour of cloud, over 99% of the SO_2 initially present has been depleted by aqueous-phase oxidation of S(IV). Figure 8 shows the contribution of the different oxidants to the oxi-

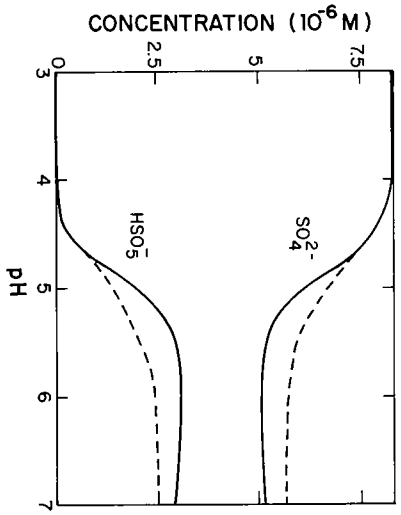

Fig. 9. Concentrations of SO_4^{2-} and HSO_5^- 1 hour after cloud formation, as a function of cloud water *p*H. Reaction is assumed to proceed either by branch (RA81*a*) (solid line), or by branches (RA81*b*) or (RA81*c*) (dashed line). Branches (RA81*b*) and (RA81*c*) give identical results. Model conditions are those of Table 1.

dation of S(IV), as a function of cloud water *p*H. At low *p*H (condensation on acid nuclei) the only important oxidant is H_2O_2(aq), because the reaction $H_2O_2 + HSO_3^-$ is acid catalyzed [*McArdle and Hoffmann*, 1983]. At high *p*H (condensation on alkaline nuclei), S(IV) is oxidized by O_3(aq) and OH(aq) more rapidly than by H_2O_2.

The intrinsic rate of oxidation of S(IV) by O_3(aq) is first order in SO_3^{2-} concentration, and therefore the rate increases rapidly with increasing *p*H. However, the actual reaction rate becomes increasingly limited at high *p*H by the rate of aqueous-phase diffusion of O_3(aq). Because of this mass transport limitation in the rate of oxidation of S(IV) by O_3(aq), OH(aq) remains an important S(IV) oxidant even at high *p*H. Above *p*H 6 it is predicted that the main S(IV) species oxidized by OH(aq) is HMSA, which is formed rapidly in the initial stage of the cloud and is not oxidized by O_3(aq).

The only sulfur species present in significant concentrations 1 hour after cloud formation are SO_4^{2-} and HSO_5^-. Figure 9 shows the concentrations of both species, as a function of cloud water *p*H. Under acidic conditions only SO_4^{2-} is formed, because H_2O_2(aq) is the only important S(IV) oxidant. Above *p*H 5, however, oxidation of S(IV) by OH(aq) produces substantial amounts of HSO_5^-. In the *p*H range 5.5–7, HSO_5^- constitutes about 35% of total cloud water sulfur. Peroxymonosulfate is reduced to SO_4^{2-} by oxidation of HSO_3^-, but this reaction is inhibited as SO_2 is depleted rapidly in the cloud by reaction of S(IV) with other oxidants (in particular, O_3(aq)). Therefore HSO_5^- is not depleted over the lifetime of the cloud. A steady state between SO_5^- and HSO_5^- is eventually approached:

$$\text{(RA82)} \qquad SO_5^- + O_2^- \xrightarrow{H_2O} HSO_5^- + OH^- + O_2$$

$$\text{(RA87)} \qquad HSO_5^- + OH \rightarrow SO_5^- + H_2O$$

Figure 9 indicates that the amount of HSO_5^- produced is only weakly dependent on the branching ratio of (RA81), $SO_5^- + HSO_3^-$. This is because (RA82), $SO_5^- + O_2^-$, is a faster sink for SO_5^- than (RA81). Reaction (RA81), propagating the S(IV) oxidation chain, is important only in the very early stage of the cloud when the HSO_3^- concentration is high. This is illustrated by Figure 8: the initiation step in the chain, reaction OH + S(IV), is a more important contributor to S(IV) oxidation than the propagation step, reaction $SO_5^- + HSO_3^-$. (RA81*b*) and (RA81*c*) give identical results because SO_4^- is removed by oxidation of Cl^- and H_2O_2(aq) and does not propagate the chain oxidation of S(IV). The main sinks for Cl_2^-, produced by the reaction $SO_4^- + Cl^-$ are the reactions with H_2O_2 and $O_2(-I)$.

SENSITIVITY TO MODEL CONDITIONS

Changes in Radiation Field

The sensitivity of the chemistry to changes in radiation field upon cloud formation was investigated by running two simulations in which the *J* values were assumed to change upon cloud formation by +50% in one case, and −50% in the other case (other model conditions as given in Table 1). Results are shown in Table 4.

The concentrations of OH(g) and OH(aq) respond almost linearly to changes in the radiation field. This is because the main sources of these species are the photolysis reactions of O_3 and H_2O_2. The concentrations of HO_2 species show a weaker response to changes in radition field, even though the main source of HO_2 is the conversion $OH(g) \rightarrow HO_2(g)$. The reason for this weaker response of HO_2 species is that the main HO_2 sink in cloud, aqueous-phase reaction $HO_2 + O_2^-$, is second order in HO_2 concentration. Therefore an increase in the HO_2 source is moderated by a higher-order increase in the HO_2 sink.

The HCOOH concentration increases with a stronger radiation field because of the increase in the OH(aq) concentration. However, the dependence of the HCOOH concentration on the radiation field is itself strongly dependent on cloud water *p*H. At low *p*H, when HCOOH produced by the aqueous-phase reaction $H_2C(OH)_2 + OH$ is volatilized, the concentration of HCOOH responds linearly to changes in the radiation field in the same way as the concentration of OH(aq). On the other hand, at high *p*H, HCOOH is mostly present as $HCOO^-$, which follows (21); the dependence of the HCOOH concentration on the radiation field then follows that of the CH_2O concentration, which is very weak.

Sticking Coefficient, Droplet Radius

A series of simulations was conducted with the standard conditions of Table 1, but with α ranging from 10^{-4} to 1 (the

TABLE 4. Effect of Changes in the Radiation Field

Species	Change in *J* Values Upon Cloud Formation: −50%	0%	+50%
	Concentration, molecules cm^{-3} air		
OH(g)	2.0(6)	3.9(6)	5.9(6)
HO_2(g)	1.2(8)	1.7(8)	2.1(8)
$HCOOH_T$	2.0(9)	2.9(9)	3.5(9)
CH_2O_T[a]	1.2(10)	1.2(10)	1.1(10)
	Concentration, M		
OH(aq)	2.5(−13)	4.1(−13)	5.6(−13)
$O_2(-I)$	1.7(−8)	2.3(−8)	2.9(−8)

Read 2.0(6) as 2.0×10^6. Other conditions are as in Table 1; concentrations are taken 1 hour after cloud formation.

[a]The value $n_{CH_2O_T} = n_{CH_2O(g)} + 6.023 \times 10^{20} L [H_2C(OH)_2]$.

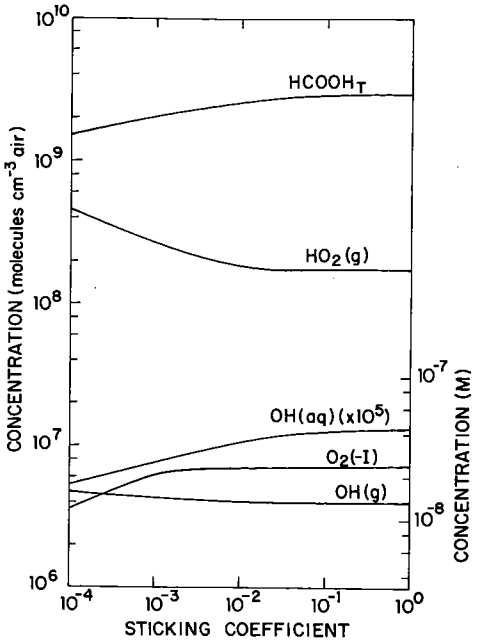

Fig. 10. Concentrations of OH, HO_2, and $HCOOH_T$ 1 hour after cloud formation, as a function of sticking coefficient. Other model conditions are those of Table 1. Gas-phase and $HCOOH_T$ concentrations are in units of molecules per cubic centimeter of air (left-hand scale), and aqueous-phase concentrations are in units of moles per liter of water (right-hand scale). Both scales are equivalent (equation (14)).

same value of α was assumed for all gases). Results are shown in Figure 10. The cloud water pH is controlled by the scavenging of very soluble gases (HNO_3, HCl, NH_3) in the initial stage of the cloud. The time required for 95% scavenging of infinitely soluble gases increases from 20 s for $\alpha = 1$ to 40 min for $\alpha = 1 \times 10^{-4}$ [*Jacob*, 1985]. Even with $\alpha = 1 \times 10^{-4}$, a stable cloud water pH of 4.16 is reached within 1 hour following cloud formation. Therefore pH is not a factor in the dependence of concentrations on α shown in Figure 10. Note that a stable pH would not be reached after 1 hour of cloud if α was lower than 10^{-4}; however, as pointed out above, such low values are not likely in remote clouds.

Other soluble species, such as CH_2O and H_2O_2, approach Henry's law equilibrium within minutes following cloud formation, even with α as low as 10^{-4} [*Jacob*, 1985]. Therefore the concentrations of these species show little dependence on α. The concentration of OH(g) is also quite insensitive to α, because gas-droplet exchange is not a major source or sink for this species. The only gas-phase species showing a strong dependence on α is HO_2(g), whose lifetime in cloud is controlled by the rate of gas-droplet transfer (Figure 2). Concentrations of HO_2(g) are 2.7 times higher for $\alpha = 1 \times 10^{-4}$ than for $\alpha = 1$. This dependence of the HO_2(g) concentration on α is consistent with that previously predicted by *Schwartz* [1984].

The dependence of the $O_2(-I)$ concentration on α follows the dependence of the HO_2(g) source, but it is much weaker. This is partly because $O_2(-I)$ is also produced by aqueous-phase sources and partly because removal of $O_2(-I)$ by the reaction $HO_2 + O_2^-$ is a second-order sink. The concentration of OH(aq) is weakly dependent on α; this dependence is due to the flux of OH(g) to the droplets and the rate of the aqueous-phase source reaction $O_2^- + O_3$. The dependence of the HCOOH concentration on α follows that of OH(aq).

The sensitivity of the chemistry to the rate of gas-droplet transfer was further explored by a series of simulations with different droplet radii ranging from 5 to 30 μm (other conditions as in Table 1; liquid water content was held constant at 5×10^{-7} vol/vol). The continuum gas-droplet transfer flux varies as $(1/a^2)$, and the noncontinuum correction to the flux is small when $\alpha = 0.1$ (Figure 1). Changes in droplet radius and changes in α both affect only the rates of gas-droplet transfer; therefore they are interpreted in the same manner. Results are shown in Figure 11 for OH and HO_2 species and for $HCOOH_T$. The concentration of OH(aq) decreases by a factor of 3 as the droplet radius increases from 5 μm to 30 μm; the concentration of OH(g) increases by 30% over this same range.

Liquid Water Content

The sensitivity of the chemistry to L was explored by a series of simulations with L ranging from 1×10^{-7} to 1.5×10^{-6} vol/vol (other model conditions as in Table 1). As L increases, gas-droplet transfer fluxes increase because of the larger liquid water surface area. Further, the equilibrium partitioning of a soluble species between the gas phase and the aqueous phase is shifted towards the aqueous phase. Aqueous-phase concentrations (M) generally decrease because of the higher dilution; the pH of the cloud rises from 3.48 with $L = 1 \times 10^{-7}$ vol/vol to 4.61 with $L = 1.5 \times 10^{-6}$ vol/vol.

Results are shown in Figure 12 for OH and HO_2 species and for $HCOOH_T$. The HO_2(g) concentration decreases rapidly with increasing L because of the increase in the droplet sink. Scavenging of HO_2(g) by the droplets is enhanced both

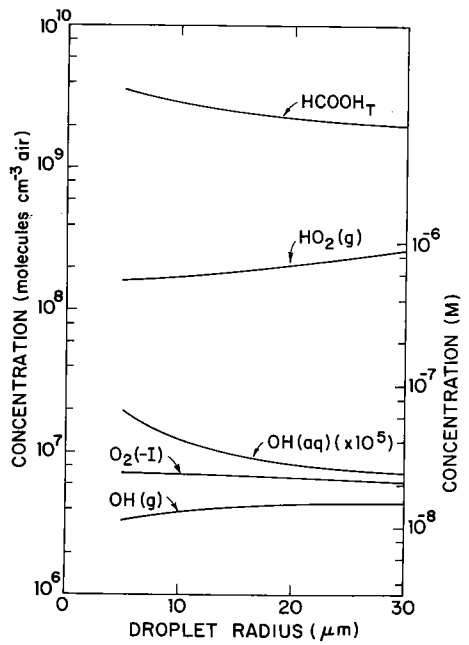

Fig. 11. Concentrations of OH, HO_2, and $HCOOH_T$ 1 hour after cloud formation, as a function of droplet radius (constant liquid water content). Other model conditions are those of Table 1. Gas-phase and $HCOOH_T$ concentrations are in units of molecules per cubic centimeter of air (left-hand scale), and aqueous-phase concentrations are in units of moles per liter of water (right-hand scale). Both scales are equivalent (equation (14)).

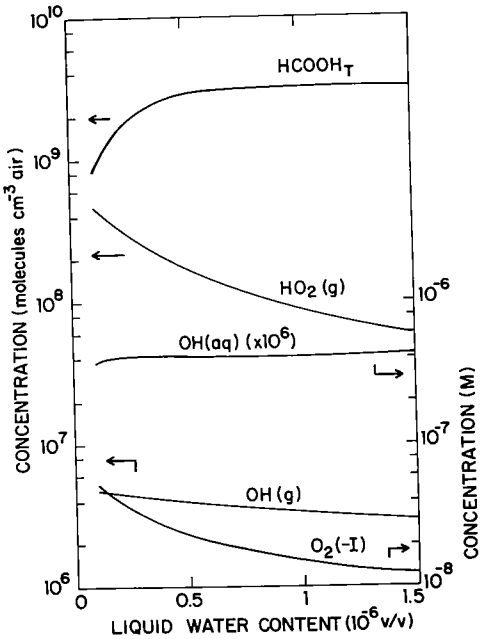

Fig. 12. Concentrations of OH, HO_2, and $HCOOH_T$ 1 hour after cloud formation, as a function of liquid water content (constant droplet radius). Other model conditions are those of Table 1. Gas-phase and $HCOOH_T$ concentrations are in units of molecules per cubic centimeter of air (left-hand scale), and aqueous-phase concentrations are in units of moles per liter of water (right-hand scale). The two scales are not equivalent because the liquid water content is not constant.

by the increase in the gas-droplet transfer flux and by the rise in *p*H, which favors HO_2(aq) dissociation in the aqueous phase. The dissociation of HO_2(aq) enhances the $O_2(-I)$ sink; therefore the $O_2(-I)$ concentration (M) decreases with increasing L. The concentration of OH(g) decreases slightly with increasing L, for two major reasons: (1) increased scavenging of H_2O_2(g) inhibits the $H_2O_2 + h\nu$ source, and (2) transfer of OH(g) to the droplets is faster. The decrease in the concentration of OH(g) lowers the gas-phase source of OH(aq), but on the other hand, the aqueous-phase source of OH(aq) (RA27) rises because of the increase in *p*H (see above). These opposite effects balance one another, so that the OH(aq) concentration (M) shows very little sensitivity to liquid water content. The concentration of $HCOOH_T$ increases rapidly with increasing L up to 5×10^{-7} vol/vol, because of enhanced scavenging of CH_2O by cloud. The *p*H of the cloud is low, therefore HCOOH is stabilized by volatilization to the gas phase. For $L > 5 \times 10^{-7}$ vol/vol, however, volatilization of HCOOH to the gas phase is restricted both by the rise in *p*H and by the increasing amount of liquid water present; this increases the efficiency of the aqueous-phase sink, reaction $HCOO^- + OH$. As a result, the $HCOOH_T$ concentration shows little dependence on L above 5×10^{-7} vol/vol.

CONCLUSIONS

A detailed gas-phase/aqueous-phase cloud chemistry model has been developed which takes into account the radial dependence of the concentrations of short-lived aqueous-phase species. The model is applied to the study of OH chemistry in a remote marine tropical cloud. The main sources of OH(aq) are the aqueous-phase reactions $O_2^- + O_3$ and $H_2O_2 + h\nu$ and the absorption of OH(g). The main sinks are the oxidation of $H_2C(OH)_2$, H_2O_2(aq), and $HCOO^-$. The concentration of OH(aq) increases with increasing cloud water *p*H but shows little dependence on liquid water content, droplet radius, or sticking coefficient. The chemical lifetime of OH(aq) is of the order of 10^{-4} s, which is too short to allow for mixing within the droplets. Therefore a strong OH(aq) concentration gradient exists between the interior and the surface of the droplets. The concentration of OH(aq) away from the droplet surface is given by an aqueous-phase chemical steady state independent of OH gas-droplet transfer.

Scavenging of OH(g) by cloud droplets must be modeled as a reversible process, that is, one cannot assume that the droplets behave as diffusion-limited sinks for OH(g). The OH flux is generally directed from the gas phase to the aqueous phase, but a net OH flux out of the droplets is found when aqueous-phase production of OH(aq) is very rapid (for example, at high *p*H). Cloud formation is found to cause a 25% decrease in the OH(g) concentration, mostly because scavenging of HO_2(g) and H_2O_2(g) interrupts the gas-phase odd hydrogen cycle. The concentration of OH(g) in cloud shows little dependence on cloud water *p*H, liquid water content, droplet radius, or sticking coefficient.

The effect of aqueous-phase radical chemistry on the CH_4 oxidation chain in cloud has been investigated. The main feature of this chemistry is the rapid aqueous-phase production of HCOOH; the efficiency of a cloud as a source of HCOOH is shown to be strongly dependent on cloud water *p*H. At $pH < 5$, HCOOH produced in the aqueous phase is volatilized to the gas phase, where it has a long lifetime against oxidation by OH(g). At $pH > 5$, however, HCOOH remains in the aqueous phase as $HCOO^-$ and is rapidly oxidized by OH(aq). Therefore clouds with $pH > 5$ are not efficient sources of HCOOH. Production of HCOOH is most efficient at $pH \approx 3.5$. The concentration of $HCOO^-$ is highest at $pH \approx 5$. Concentrations of HCOOH species shows little dependence on droplet radius or sticking coefficient and little dependence on liquid water content above 5×10^{-7} vol/vol.

A novel mechanism has been proposed for the oxidation of S(IV) by OH(aq) in remote clouds. It is predicted from this mechanism that the intermediate SO_5^- does not propagate a S(IV) oxidation chain by the reaction $SO_5^- + HSO_3^-$ but reacts instead with O_2^- to produce HSO_5^- (peroxymonosulfate). At cloud water *p*H values above 5, HSO_5^- is found to contribute about 35% of total cloud water sulfur (the remainder being contributed by SO_4^{2-}). At this date, no attempts have been made to determine HSO_5^- concentrations in cloud water samples. It is hoped that this model study will encourage such attempts.

Acknowledgments. S. C. Wofsy and M. J. Prather provided inspiration and many stimulating discussions. I thank J. A. Logan and M. B. McElroy for their careful review of the manuscript and C. Spivakovsky for her advice on the mathematics. Valuable discussions with M. R. Hoffmann, R. E. Huie, and C. J. Walcek are gratefully acknowledged. This research was supported by funds from the National Aeronautics and Space Administration (grant NAGW-731) and from the National Science Foundation (grant ATM-83-17009).

REFERENCES

Adams, G. E., and J. W. Boag, Spectroscopic studies of reactions of the OH radical, *Proc. Chem. Soc. London*, 112, 1964.

Adewuyi, Y. G., S.-Y. Cho, R.-P. Tsay, and G. R. Carmichael, Importance of formaldehyde in cloud chemistry, *Atmos. Environ.*, *18*, 2413–2420, 1984.

Anbar, M., and P. Neta, A compilation of specific bimolecular rate constants for the reactions of hydrated electrons, hydrogen atoms and hydroxyl radicals with inorganic and organic compounds in aqueous solution, *Int. J. Appl. Radiat. Isot., 18*, 493–523, 1967.

Atkinson, R., and A. C. Lloyd, Evaluation of kinetic and mechanistic data for modeling of photochemical smog, *J. Phys. Chem. Ref. Data, 13*, 315–444, 1984.

Ayers, G. P., and J. L. Gras, The concentration of ammonia in southern ocean air, *J. Geophys. Res., 88*, 10,655–10,659, 1983.

Baxendale, J. H., M. D. Ward, and P. Wardman, Heats of ionization of HO_2 and OH in aqueous solution, *Trans. Farad. Soc., 67*, 2532–2537, 1971.

Behar, D., G. Czapski, and I. Duchovny, Carbonate radical in flash photolysis and pulse radiolysis of aqueous carbonate solutions, *J. Phys. Chem., 74*, 2206–2210, 1970.

Bell, R. P., The reversible hydration of carbonyl compounds, *Adv. Phys. Org. Chem., 4*, 1–29, 1966.

Bielski, B. H. J., Reevaluation of the spectral and kinetic properties of HO_2 and O_2^- free radicals, *Photochem. Photobiol., 28*, 645–649, 1978.

Bothe, E., and D. Schulte-Frohlinde, Reaction of dihydroxymethyl radical with molecular oxygen in aqueous solution, *Z. Naturforsch. B, Anorg. Chem. Org. Chem., 35*, 1035–1039, 1980.

Boyce, S. D., and M. R. Hoffmann, Kinetics and mechanism of the formation of hydroxymethanesulfonic acid at low *p*H, *J. Phys. Chem., 88*, 4740–4746, 1984.

Buhler, R. E., J. Staehelin, and J. Hoigne, Ozone decomposition in water studied by pulse radiolysis, 1, HO_2/O_2^- and HO_3/O_3^- as intermediates, *J. Phys. Chem., 88*, 2560–2564, 1984.

Calvert, J. G., and W. R. Stockwell, Mechanisms and rates of the gas-phase oxidations of sulfur dioxide and nitrogen oxides in the atmosphere, in *SO_2, NO and NO_x Oxidation Mechanisms: Atmospheric Considerations, Acid Precipitation Ser.*, vol. 3, edited by J. G. Calvert, pp. 1–62, Butterworth, Stoneham, Mass., 1984.

Cavanagh, L. A., C. F. Schadt, and E. Robinson, Atmospheric hydrocarbon and carbon monoxide measurements at Point Barrow, Alaska, *Environ. Sci. Technol., 3*, 251–257, 1969.

Chameides, W. L., The photochemistry of a remote marine stratiform cloud, *J. Geophys. Res., 89*, 4739–4755, 1984.

Chameides, W. L., Reply, *J. Geophys. Res., 90*, 5865, 1985.

Chameides, W. L., and D. D. Davis, The free radical chemistry of cloud droplets and its impact upon the composition of rain, *J. Geophys. Res., 87*, 4863–4877, 1982.

Chameides, W. L., and A. Tan, The two-dimensional diagnostic model for tropospheric OH: An uncertainty analysis, *J. Geophys. Res., 86*, 5209–5223, 1981.

Chao, J., and B. J. Zwolinski, Ideal gas thermodynamic properties of methanoic and ethanoic acids, *J. Phys. Chem. Ref. Data, 7*, 363–377, 1978.

Chen, S., V. W. Cope, and M. Z. Hoffman, Behavior of CO_3^- radicals generated in the flash photolysis of carbonatoamines complexes of cobalt(III) in aqueous solution, *J. Phys. Chem., 77*, 1111–1116, 1973.

Christensen, H., K. Sehested, and H. Corfitzen, Reactions of hydroxyl radicals with hydrogen peroxide at ambient and elevated temperatures, *J. Phys. Chem., 86*, 1588–1590, 1982.

Damschen, D. E., and L. R. Martin, Aqueous aerosol oxidation of nitrous acid by O_2, O_3, and H_2O_2, *Atmos. Environ., 17*, 2005–2011, 1983.

Daniels, M., Radiolysis and photolysis of the aqueous nitrate system. *Adv. Chem. Ser., 81*, 153–163, 1968.

Deister, U., V. R. Neeb, J. Helas, and P. Warneck, The equilibrium of $CH_2[OH]_2 + HSO_3^- \rightleftarrows CH_2[OH]SO_3^-$ in aqueous solution: Temperature dependence and importance in cloud, *J. Phys. Chem.*, in press, 1986.

Devuyst, E. A. P., V. A. Ettel, and M. A. Mosoiu, An oxidant of unexpected utility, *Chemtech*, 426–427, 1979.

Dogliotti, L., and E. Hayon, Flash photolysis of persulfate ions in aqueous solutions. Study of the sulfate and ozonide radical ions, *J. Phys. Chem., 71*, 2511–2516, 1967.

Dogliotti, L., and E. Hayon, Flash photolysis study of sulfite, thiocyanate and thiosulphate ions in solution, *J. Phys. Chem., 72*, 1800–1807, 1968.

Edwards, J. O., *Inorganic Reaction Mechanisms*, p. 84, W. A. Benjamin, New York, 1964.

Edwards, J. O., and J. J. Mueller, The rates of oxidation of nitrite ion by several peroxides, *Inorg. Chem., 1*, 696–699, 1962.

Fortnum, D. H., C. J. Battaglia, S. R. Cohen, and J. O. Edwards, The kinetics of the oxidation of halide ions by monosubstituted peroxides, *J. Am. Chem. Soc., 82*, 778–782, 1960.

Fuchs, N. A., and A. G. Sutugin, High-dispersed aerosols, in *International Reviews of Aerosol Physics and Chemistry*, vol. 2, edited by G. M. Hidy and J. R. Brock, pp. 1–60, Pergamon, New York, 1971.

Gill, P. S., T. E. Graedel, and C. J. Wechsler, Organic films on atmospheric aerosol particles, fog droplets, cloud droplets, raindrops, and snowflakes, *Rev. Geophys., 21*, 903–920, 1983.

Gillette, D. A., and I. H. Blifford, Jr., Composition of tropospheric aerosols as a function of altitude, *J. Atmos. Sci., 28*, 1199–1210, 1971.

Glasstone, S., K. J. Laidler, and H. Eyring, *The Theory of Rate Processes*, p. 523, McGraw-Hill, New York, 1941.

Graedel, T. E., and K. I. Goldberg, Kinetic studies of raindrop chemistry, 1, Inorganic and organic processes, *J. Geophys. Res., 88*, 10,865–10,882, 1983.

Graedel, T. E., and C. J. Wechsler, Chemistry within aqueous aerosols and raindrops, *Rev. Geophys., 19*, 505–539, 1981.

Gratzel, M., A. Henglein, and S. Taniguchi, Pulsradiolytische Beobachtungen uber die reduktion des NO_3^--Ions und uber Bildung und Zerfall des persalpetrigen Saure in wassriger Losung, *Ber. Bunsenges. Phys. Chem., 74*, 292–298, 1970.

Hagesawa, K., and P. Neta, Rate constants and mechanisms of reaction for Cl_2^- radicals, *J. Phys. Chem., 82*, 854–857, 1978.

Hales, J. M., and D. R. Drewes, Solubility of ammonia in water at low concentrations, *Atmos. Environ., 13*, 1133–1147, 1979.

Hayon, E., A. Treinin, and J. Wilf, Electronic spectra, photochemistry, and autoxidation mechanism of the sulfite-bisulfite-pyrosulfite systems; The SO_2^-, SO_3^-, SO_4^-, and SO_5^- radicals, *J. Am. Chem. Soc., 94*, 47–57, 1972.

Hegg, D. A., The importance of liquid-phase oxidation of SO_2 in the troposphere, *J. Geophys. Res., 90*, 3773–3779, 1985.

Hoffmann, M. R., Thermodynamic, kinetic, and extrathermodynamic considerations in the development of equilibrium models for aquatic systems, *Environ. Sci. Technol., 15*, 345–353, 1981.

Hoffmann, M. R., On the kinetics and mechanism of oxidation of aquated sulfur dioxide by ozone, *Atmos. Environ.*, in press, 1986.

Hoffmann, M. R., and J. G. Calvert, Chemical transformation modules for Eulerian acid deposition models, vol. 2, The aqueous-phase chemistry, *Rep. EPA/600/3-85/017*, Environ. Prot. Agency, Research Triangle Park, N. C., 1985.

Hoigne, J., and H. Bader, Rate constants of reactions of ozone with organic and inorganic compounds in water, 1, Non-dissociating organic compounds, *Water Res., 17*, 173–183, 1983*a*.

Hoigne, J., and H. Bader, Rate constants of reactions of ozone with organic and inorganic compounds in water, 2, Dissociating organic compounds, *Water Res., 17*, 185–194, 1983*b*.

Hoigne, J., H. Bader, W. R. Haag, and J. Staehelin, Rate constants of reactions of ozone with organic and inorganic compounds in water, 3, Inorganic compounds and radicals, *Water Res., 19*, 993–1004, 1985.

Huie, R. E., and P. Neta, Chemical behavior of SO_3^- and SO_5^- radicals in aqueous solutions, *J. Phys. Chem., 88*, 5665–5669, 1984.

Jacob, D. J., Comment on "The photochemistry of a remote marine stratiform cloud" by William L. Chameides, *J. Geophys. Res., 90*, 5864, 1985.

Jacob, D. J., and M. R. Hoffmann, A dynamic model for the production of H^+, NO_3^-, and SO_4^{2-}, in urban fog, *J. Geophys. Res., 88*, 6611–6621, 1983.

Jacob, D. J., J. W. Munger, J. M. Waldman, and M. R. Hoffmann, The H_2SO_4-HNO_3-NH_3 system at high humidities and in fogs, 1, Spatial and temporal patterns in the San Joaquin Valley of California, *J. Geophys. Res., 91*, 1073–1088, 1986*a*.

Jacob, D. J., J. M. Waldman, J. W. Munger, and M. R. Hoffmann, The H_2SO_4-HNO_3-NH_3 system at high humidities and in fogs, 2, Comparison of field data with thermodynamic calculations, *J. Geophys. Res., 91*, 1089–1096, 1986*b*.

Jayson, G. G., B. J. Parsons, and A. J. Swallow, Some simple, highly reactive, inorganic chlorine derivatives in aqueous solution, *Trans. Farad. Soc., 69*, 1597–1607, 1973.

Jet Propulsion Laboratory, Chemical kinetics and photochemical data for use in stratospheric modeling, Evaluation 6, *JPL Publ. 83-62*, California Institute of Technology, Pasadena, 1983.

Keene, W. C., J. N. Galloway, and J. D. Holden, Jr., Measurement of weak organic acidity in precipitation from remote areas of the world, *J. Geophys. Res., 88*, 5122–5130, 1983.

Klaning, U. K., K. Sehested, and J. Holcman, Standard Gibbs free energy of formation of the hydroxyl radical in aqueous solution; Rate constants for the reaction $ClO_2^- + O_3 \rightleftarrows O_3^- + ClO_2$, *J. Phys. Chem.*, *89*, 760–763, 1985.

Kok, G. L., S. N. Gitlin, and A. L. Lazrus, Kinetics of the formation and decomposition of hydroxymethanesulfonate, *J. Geophys. Res.*, *91*, 2801–2804, 1986.

Kyrki, J., Caro's acid and its thermal hydrolysis in acid and alkaline $NaClO_4$ solutions, *Ann. Univ. Turku., Ser. A.*, *61*, 1963.

Latimer, W. M., *The Oxidation States of the Elements and their Potentials in Aqueous Solutions*, 2nd ed., pp. 45, 128, Prentice-Hall, New York, 1952.

Ledbury, W., and E. W. Blair, The partial formaldehyde vapour pressure of aqueous solutions of formaldehyde, II, *J. Chem. Soc.*, *127*, 2832–2839, 1925.

Lee, Y. N., and S. E. Schwartz, Reaction kinetics of nitrogen dioxide with liquid water at low partial pressure, *J. Phys. Chem.*, *85*, 840–848, 1981.

Levine, S. Z., and S. E. Schwartz, In-cloud and below-cloud scavenging of nitric acid vapor, *Atmos. Environ.*, *16*, 1725–1734, 1982.

Lind, J., and T. E. Eriksen, Pulse radiolysis of methane sulphonic acid, *Radiochem. Radioanal. Lett.*, *21*, 177–181, 1975.

Lind, J. A., and G. L. Kok, Henry's law determinations for aqueous solutions of hydrogen peroxide, methylhydroperoxide, and peroxyacetic acid, *J. Geophys. Res.*, *91*, 7889–7895, 1986.

Logan, J. A., M. J. Prather, S. C. Wofsy, and M. B. McElroy, Tropospheric chemistry: A global perspective, *J. Geophys. Res.*, *86*, 7210–7254, 1981.

Maroulis, P. J., A. L. Torres, A. B. Goldberg, and A. R. Bandy, Atmospheric SO_2 measurements on project GAMETAG, *J. Geophys. Res.*, *85*, 7345–7349, 1980.

Maruthamuthu, P., and P. Neta, Radiolytic chain decomposition of peroxomonophosphoric and peroxomonosulfuric acids, *J. Phys. Chem.*, *81*, 937–940, 1977.

Maruthamuthu, P., and P. Neta, Phosphate radicals, Spectra, acid-base equilibria, and reactions with inorganic compounds, *J. Phys. Chem.*, *82*, 710–713, 1978.

McArdle, J. V., and M. R. Hoffmann, Kinetics and mechanism of the oxidation of aquated sulfur dioxide by hydrogen peroxide at low *p*H, *J. Phys. Chem.*, *87*, 5425–5429, 1983.

McElroy, W. J., The aqueous oxidation of SO_2 by OH radicals, *Atmos. Environ.*, *20*, 323–330, 1986.

Munger, J. W., D. J. Jacob, and M. R. Hoffmann, The occurrence of bisulfite-aldehyde addition products in fog- and cloudwater, *J. Atmos. Chem.*, *1*, 335–350, 1984.

Munger, J. W., C. Tiller, and M. R. Hoffmann, Identification of hydroxymethanesulfonate in fogwater, *Science*, *231*, 247–249, 1986.

National Bureau of Standards, JANAF Thermodynamic Tables, 2nd ed., *NSRDS-NBS 37*, U. S. Dep. of Commerce, Washington, D. C., 1971.

National Research Council, *Global Tropospheric Chemistry: A Plan for Action*, National Academy Press, Washington, D. C., 1984.

Pruppacher, H. R., and J. D. Klett, *Microphysics of Clouds and Precipitation*, pp. 133, 421, D. Reidel, Hingham, Mass., 1978.

Rettich, T. R., Some photochemical reactions of aqueous nitric acid, *Diss. Abstr. Int. B*, *38*, 5968, 1978.

Richtmeyer, R. D., *Difference Methods for Initial Value Problems*, p. 101, Wiley-Interscience, New York, 1957.

Ross, A. B., and P. Neta, Rate constants for reactions of inorganic radicals in aqueous solution, *Rep. NSRDS-NBS 65*, U.S. Dept. of Commerce, Washington, D. C., 1979.

Rudolph, J., and D. H. Ehhalt, Measurements of C_2-C_5 hydrocarbons over the North Atlantic, *J. Geophys. Res.*, *86*, 11,959–11,964, 1981.

Saltzman, E. S., D. L. Savoie, R. G. Zika, and J. M. Prospero, Methane sulfonic acid in the atmosphere, *J. Geophys. Res.*, *88*, 10,897–10,902, 1983.

Schwartz, S. E., Gas- and aqueous-phase chemistry of HO_2 in liquid water clouds, *J. Geophys. Res.*, *89*, 11,589–11,598, 1984.

Schwartz, S. E., Mass-transport considerations pertinent to aqueous-phase reactions of gases in liquid-water clouds, in *Chemistry of Multiphase Atmospheric Systems*, edited by W. Jaeschke, vol. G6, pp. 415–471, Springer-Verlag, New York, 1986.

Schwartz, S. E., and J. E. Freiberg, Mass-transport limitation to the rate of reaction of gases in liquid droplets: application to oxidation of SO_2 in aqueous solutions, *Atmos. Environ.*, *15*, 1129–1144, 1981.

Schwartz, S. E., and W. H. White, Solubility equilibria of the nitrogen oxides and oxyacids in aqueous solution, *Adv. Environ. Sci. Eng.*, *4*, 1–45, 1981.

Sehested, K., O. L. Rasmussen, and H. Fricke, Rate constants of OH with HO_2, O_2^-, and $H_2O_2^+$ from hydrogen peroxide formation in pulse-irradiated oxygenated water, *J. Phys. Chem.*, *72*, 626–631, 1968.

Sehested, K., J. Holcman, and E. J. Hart, Rate constants and products of the reactions of e_{aq}^-, O_2^-, and H with ozone in aqueous solutions, *J. Phys. Chem.*, *87*, 1951–1954, 1983.

Sehested, K., J. Holcman, E. Bjergbakke, and E. J. Hart, A pulse radiolytic study of the reaction $OH + O_3$ in aqueous medium, *J. Phys. Chem.*, *88*, 4144–4147, 1984.

Seigneur, C., and P. Saxena, A study of atmospheric acid formation in different environments, *Atmos. Environ.*, *18*, 2109–2124, 1984.

Seigneur, C., P. Saxena, and V. A. Mirabella, Diffusion and reaction of pollutants in stratus clouds: Application to nocturnal acid formation in plumes, *Environ. Sci. Technol.*, *19*, 821–828, 1985.

Shapilov, O. D., and Y. L. Kostyukovskii, Reaction kinetics of hydrogen peroxide with formic acid in aqueous solutions, *Kinet. Katal.*, *15*, 1065–1067, 1974.

Sillen, G. L., and A. E. Martell, Stability constants of metal-ion complexes, *Spec. Publ. Chem. Soc.*, *17*, 357, 1964.

Snider, J. R., and G. A. Dawson, Tropospheric light alcohols, carbonyls, and acetonitrile: Concentrations in the southwestern United States and Henry's law data, *J. Geophys. Res.*, *90*, 3797–3805, 1985.

Sorensen, P. E., and V. S. Andersen, The formaldehyde-hydrogen sulphite system in alkaline aqueous solution: kinetics, mechanism, and equilibria, *Acta Chem. Scand.*, *24*, 1301–1306, 1970.

Staehelin, J., and J. Hoigne, Decomposition of ozone in water: Rate of initiation by hydroxide ions and hydrogen peroxide, *Environ. Sci. Technol.*, *16*, 676–681, 1982.

Staehelin, J., R. E. Buhler, and J. Hoigne, Ozone decomposition in water studied by pulse radiolysis, 2, OH and HO_4 as chain intermediates, *J. Phys. Chem.*, *88*, 5999–6004, 1984.

Steele, W. V., and E. H. Appelman, The standard enthalpy of formation of peroxymonosulfate (HSO_5^-) and the standard electrode potential of the peroxymonosulfate-bisulfate couple, *J. Chem. Thermodyn.*, *14*, 337–344, 1982.

Stockwell, W. R., and J. G. Calvert, The mechanism of NO_3 and HONO formation in the nighttime chemistry of the urban atmosphere, *J. Geophys. Res.*, *88*, 6673–6682, 1983.

Su, F., J. G. Calvert, and J. H. Shaw, Mechanism of the photooxidation of gaseous formaldehyde, *J. Phys. Chem.*, *83*, 3185–3191, 1979.

Thomas, J. R., and K. U. Ingold, Determination of rate constants for the self-reactions of peroxy radicals by electron spin resonance spectroscopy, *Adv. Chem. Ser.*, *75*, 258–268, 1968.

Treinin, A., The photochemistry of oxyanions, *Isr. J. Chem.*, *8*, 103–113, 1970.

Vierkorn-Rudolph, B., K. Bachmann, and B. Schwarz, Vertical profiles of hydrogen chloride in the troposphere, *J. Atmos. Chem.*, *2*, 47–63, 1984.

Wagman, D. D., W. H. Evans, V. B. Parker, R. H. Schumm, I. Halow, S. M. Bailey, K. L. Churney, and R. L. Nuttall, The NBS tables of chemical thermodynamic properties; Selected values for inorganic and C_1 and C_2 organic substances in SI units, *J. Phys. Chem. Ref. Data Suppl.*, *11*, suppl. 2, 1982.

Walling, C., Fenton's reagent revisited, *Acc. Chem. Res.*, *8*, 125–131, 1975.

Weeks, J. L., and J. Rabani, The pulse radiolysis of deaerated aqueous carbonate solutions, I, Transient optical spectrum and mechanism; II, *p*K for OH radicals, *J. Phys. Chem.*, *70*, 2100–2106, 1966.

Weinstein, J., and B. H. J. Bielski, Kinetics of the interaction of HO_2 and O_2^- radicals with hydrogen peroxide; The Haber-Weiss reaction, *J. Am. Chem. Soc.*, *101*, 58–62, 1979.

Zetzsch, C., and F. Stuhl, Rate constants for reactions of OH with carbonic acids, in *Proceedings of 2nd European Symposium on Physico-Chemical Behavior of Atmospheric Pollutants*, pp. 129–137, D. Reidel, Hingham, Mass., 1982.

D. Jacob, Center for Earth and Planetary Physics, Harvard University, 29 Oxford Street, Cambridge, MA 02138.

(Received December 17, 1985;
revised May 6, 1986;
accepted May 15, 1986.)